THE EUROPEAN
PHYSICAL JOURNAL C

Measurement of single-diffractive dijet production in proton–proton collisions at $\sqrt{s} = 8$ TeV with the CMS and TOTEM experiments

CMS and TOTEM Collaborations[*]

CERN, 1211 Geneva 23, Switzerland

Abstract Measurements are presented of the single-diffractive dijet cross section and the diffractive cross section as a function of the proton fractional momentum loss ξ and the four-momentum transfer squared t. Both processes pp $\rightarrow$ pX and pp $\rightarrow$ Xp, i.e. with the proton scattering to either side of the interaction point, are measured, where X includes at least two jets; the results of the two processes are averaged. The analyses are based on data collected simultaneously with the CMS and TOTEM detectors at the LHC in proton–proton collisions at $\sqrt{s} = 8$ TeV during a dedicated run with $\beta^* = 90$ m at low instantaneous luminosity and correspond to an integrated luminosity of 37.5 nb^{-1}. The single-diffractive dijet cross section σ_{jj}^{pX}, in the kinematic region $\xi < 0.1$, $0.03 < |t| < 1$ GeV^2, with at least two jets with transverse momentum $p_T > 40$ GeV, and pseudorapidity $|\eta| < 4.4$, is 21.7 ± 0.9 (stat) $^{+3.0}_{-3.3}$ (syst) ± 0.9 (lumi) nb. The ratio of the single-diffractive to inclusive dijet yields, normalised per unit of ξ, is presented as a function of x, the longitudinal momentum fraction of the proton carried by the struck parton. The ratio in the kinematic region defined above, for x values in the range $-2.9 \leq \log_{10} x \leq -1.6$, is $R = (\sigma_{jj}^{pX}/\Delta\xi)/\sigma_{jj} = 0.025 \pm 0.001$ (stat) ± 0.003 (syst), where σ_{jj}^{pX} and σ_{jj} are the single-diffractive and inclusive dijet cross sections, respectively. The results are compared with predictions from models of diffractive and nondiffractive interactions. Monte Carlo predictions based on the HERA diffractive parton distribution functions agree well with the data when corrected for the effect of soft rescattering between the spectator partons.

[*] e-mail: cms-publication-committee-chair@cern.ch

1 Introduction

In proton–proton (pp) collisions a significant fraction of the total cross section is attributed to diffractive processes. Diffractive events are characterised by at least one of the two incoming protons emerging from the interaction intact or excited into a low-mass state, with only a small energy loss. These processes can be explained by the exchange of a virtual object, the so-called Pomeron, with the vacuum quantum numbers [1]; no hadrons are therefore produced in a large rapidity range adjacent to the scattered proton, yielding a so-called large rapidity gap (LRG). A subleading exchange of Reggeons, as opposed to a Pomeron, also contributes to diffractive scattering, especially for large values of the proton fractional momentum loss ξ, and is required to describe diffractive data [2–5]. While Pomerons mainly consist of gluons, Reggeons are mesons composed of a quark–antiquark pair.

Hard diffraction has been studied in hadron-hadron collisions at the SPS at CERN [6], the Tevatron at Fermilab [7–11], the CERN LHC [12,13], and in electron–proton (ep) collisions at the HERA collider at DESY [2–5,14]. Hard diffractive processes can be described in terms of the convolution of diffractive parton distribution functions (dPDFs) and hard scattering cross sections, which can be calculated in perturbative quantum chromodynamics (pQCD). The dPDFs have been determined by the HERA experiments [2,4,5] by means of fits to inclusive diffractive deep inelastic scattering data. The dPDFs have been successfully applied to describe different hard diffractive processes in ep collisions. This success is based on the factorisation theorem proven for ep interactions at large Q^2, and on the validity of the QCD evolution equations for the dPDFs [15–17]. However, in hard diffractive hadron-hadron collisions factorisation is broken because of the presence of soft rescattering between the spectator partons. This leads to a suppression of the observed diffractive cross section in hadron-hadron collisions [18]. The suppres-

sion factor, often called the rapidity gap survival probability ($\langle S^2 \rangle$), is ∼10% at the Tevatron energies [9].

Experimentally, diffractive events can be selected either by exploiting the presence of an LRG or by measuring the scattered proton. The latter method is superior since it gives a direct measurement of t, the squared four momentum transfer at the proton vertex, and suppresses the contribution from events in which the proton dissociates into a low-mass state. The CMS Collaboration has previously reported a measurement of diffractive dijet production at $\sqrt{s} = 7$ TeV [12] that did not include information on the scattered proton. The ATLAS Collaboration has also measured dijet production with large rapidity gaps at $\sqrt{s} = 7$ TeV [13].

This article presents a measurement of dijet production with a forward, high longitudinal momentum proton at $\sqrt{s} = 8$ TeV. It corresponds to the processes pp → pX or pp → Xp, i.e. with the proton scattering to either side of the interaction and X including at least two jets. The system X is measured in CMS and the scattered proton in the TOTEM roman pots (RPs). This process is referred to as single-diffractive dijet production.

The single-diffractive dijet production cross section is measured as a function of ξ and t in the kinematic region $\xi < 0.1$ and $0.03 < |t| < 1$ GeV^2, in events with at least two jets, each with transverse momentum $p_T > 40$ GeV and pseudorapidity $|\eta| < 4.4$. The ratio of the single-diffractive to inclusive dijet cross sections is measured as a function of x, the longitudinal momentum fraction of the proton carried by the struck parton for x values in the range $-2.9 \leq \log_{10} x \leq -1.6$. This is the first measurement of hard diffraction with a measured proton at the LHC.

2 The CMS and TOTEM detectors

The central feature of the CMS apparatus is a superconducting solenoid of 6 m internal diameter, providing a magnetic field of 3.8 T. Within the superconducting solenoid volume are a silicon pixel and strip tracker, a lead tungstate crystal electromagnetic calorimeter (ECAL), and a brass and scintillator hadron calorimeter (HCAL), each composed of a barrel and two endcap sections. Forward calorimeters extend the pseudorapidity coverage provided by the barrel and endcap detectors. The forward hadron (HF) calorimeter uses steel as an absorber and quartz fibers as the sensitive material. The two HFs are located 11.2 m from the interaction region, one on each end, and together they provide coverage in the range $3.0 < |\eta| < 5.2$. Muons are measured in gas-ionisation detectors embedded in the steel flux-return yoke outside the solenoid.

When combining information from the entire detector, including that from the tracker, the jet energy resolution amounts typically to 15% at 10 GeV, 8% at 100 GeV, and 4%

at 1 TeV, to be compared to about 40, 12, and 5%, respectively, obtained when ECAL and HCAL alone are used. In the region $|\eta| < 1.74$, the HCAL cells have widths of 0.087 in pseudorapidity and 0.087 in azimuth (ϕ). In the η-ϕ plane, and for $|\eta| < 1.48$, the HCAL cells map on to 5×5 arrays of ECAL crystals to form calorimeter towers projecting radially outwards from close to the nominal interaction point. For $|\eta| > 1.74$, the coverage of the towers increases progressively to a maximum of 0.174 in $\Delta\eta$ and $\Delta\phi$. Within each tower, the energy deposits in the ECAL and HCAL cells are summed to define the calorimeter tower energies, subsequently used to provide the energies and directions of hadronic jets.

The reconstructed vertex with the largest value of summed charged-particle track p_T^2 is taken to be the primary interaction vertex. Tracks are clustered based on the z coordinate of the track at the point of closest approach to the beamline. In the vertex fit, each track is assigned a weight between 0 and 1, which reflects the likelihood that it genuinely belongs to the vertex. The number of degrees of freedom in the fit is strongly correlated with the number of tracks arising from the interaction region.

The particle-flow (PF) algorithm [19] aims to reconstruct and identify each individual particle in an event with an optimised combination of information from the various elements of the CMS detector. The energy of photons is directly obtained from the ECAL measurement, corrected for zero-suppression effects. The energy of electrons is determined from a combination of the electron momentum at the primary interaction vertex as determined by the tracker, the energy of the corresponding ECAL cluster, and the energy sum of all bremsstrahlung photons spatially compatible with originating from the electron track. The energy of muons is obtained from the curvatures of the corresponding track. The energy of charged hadrons is determined from a combination of their momentum measured in the tracker and the matching ECAL and HCAL energy deposits, corrected for zero-suppression effects and for the response function of the calorimeters to hadronic showers. Finally, the energy of neutral hadrons is obtained from the corresponding corrected ECAL and HCAL energies.

Hadronic jets are clustered from these reconstructed particles using the anti-k_T algorithm [20,21]. The jet momentum is determined as the vectorial sum of all PF candidate momenta in the jet, and is found from simulation to be within 5 to 10% of the true momentum over the whole p_T spectrum and detector acceptance. Jet energy corrections are derived from simulation, and are confirmed with in situ measurements of the energy balance in dijet, multijet, photon + jet, and Z + jet events [22]. The jet p_T resolution in the simulation is scaled upwards by around 15% in the barrel region, 40% in the endcaps and 20% in the forward region to match the resolution in the data. Additional selection criteria are applied

to each event to remove spurious jet-like features originating from isolated noise patterns in some HCAL regions [23].

A more detailed description of the CMS detector, together with a definition of the coordinate system used and the relevant kinematic variables, can be found in Ref. [24].

The TOTEM experiment [25,26] is located at the LHC interaction point (IP) 5 together with the CMS experiment. The RP system is the subdetector relevant for measuring scattered protons. The RPs are movable beam pipe insertions that approach the LHC beam very closely (few mm) to detect protons scattered at very small angles or with small ξ. The proton remains inside the beam pipe and its trajectory is measured by tracking detectors installed inside the RPs. They are organised in two stations placed symmetrically around the IP; one in LHC sector 45 (positive z), the other in sector 56 (negative z). Each station is formed by two units: near (215 m from the IP) and far (220 m from the IP). Each unit includes three RPs: one approaching the beam from the top, one from the bottom and one horizontally. Each RP hosts a stack of 10 silicon strip sensors (pitch 66 μm) with a strongly reduced insensitive region at the edge facing the beam (few tens of μm). Five of these planes are oriented with the silicon strips at a $+45°$ angle with respect to the bottom of the RP and the other five have the strips at a $-45°$ angle.

The beam optics relates the proton kinematics at the IP and at the RP location. A proton emerging from the interaction vertex (x^*, y^*) at horizontal and vertical angles θ_x^* and θ_y^*, with a fractional momentum loss ξ, is transported along the outgoing beam through the LHC magnets. It arrives at the RPs at the transverse position:

$$x(z_{RP}) = L_x(z_{RP})\,\theta_x^* + v_x(z_{RP})\,x^* - D_x(z_{RP})\,\xi,$$
$$y(z_{RP}) = L_y(z_{RP})\,\theta_y^* + v_y(z_{RP})\,y^* - D_y(z_{RP})\,\xi, \qquad (1)$$

relative to the beam centre. This position is determined by the optical functions, characterising the transport of protons in the beamline and controlled via the LHC magnet currents. The effective length $L_{x,y}(z)$, magnification $v_{x,y}(z)$ and horizontal dispersion $D_x(z)$ quantify the sensitivity of the measured proton position to the scattering angle, vertex position, and fractional momentum loss, respectively. The dispersion in the vertical plane, D_y, is nominally zero.

For the present measurement, a special beam optical setup with $\beta^* = 90$ m was used, where β^* is the value of the amplitude function of the beam at the IP. This optical setup features parallel-to-point focussing ($v_y \sim 0$) and large L_y, making y at RP directly proportional to θ_y^*, and an almost vanishing L_x and v_x, implying that any horizontal displacement at the RP is approximately proportional to ξ. Protons can hence be measured with large detector acceptance in the vertical RPs that approach the beam from the top and bottom.

To reduce the impact of imperfect knowledge of the optical setup, a calibration procedure [27] has been applied.

This method uses elastic scattering events and various proton observables to determine fine corrections to the optical functions presented in Eq. (1). For the RP alignment, a three-step procedure [26] has been applied: beam-based alignment prior to the run (as for the LHC collimators) followed by two offline steps. First, track-based alignment for the relative positions among RPs, and second, alignment with elastic events for the absolute position with respect to the beam. The final uncertainties per unit (common for top and bottom RPs) are: 2 μm (horizontal shift), 100 μm (vertical shift), and 0.2 mrad (rotation about the beam axis).

The kinematic variables ($\xi, \theta_x^*, \theta_y^*$ as well as t) are reconstructed with the use of parametrised proton transport functions [26]. The values of the optical functions vary with ξ, an effect that is taken into account by the optics parametrisation. The details of the reconstruction algorithms and optics parametrisation are discussed in Refs. [26,28]. The momentum loss reconstruction depends mostly on the horizontal dispersion, which is determined with a precision better than 10%. The scattering angle resolution depends mainly on the angular beam divergence and in the horizontal plane also on the detector resolution, whereas the momentum loss resolution depends mainly on the optics [29]. The ξ resolution is about $\sigma(\xi) = 0.7\%$ and the θ_y^* and the θ_x^* resolutions 2.4 μrad and 25 μrad, respectively.

3 Event kinematics

Figure 1 shows a schematic diagram of the single-diffractive reaction pp $\to$ Xp with X including two high-p_T jets. Single-diffractive dijet production is characterised by the presence of a high-energy proton, which escapes undetected by the CMS detector, and the system X, which contains high-p_T jets, separated from the proton by an LRG.

The proton is scattered at small angles, has small fractional momentum loss $\xi = 1 - |\mathbf{p}_f|/|\mathbf{p}_i|$, and small absolute value of the 4-momentum transfer squared $t = (p_f - p_i)^2$, where p_i and p_f are the four-momenta of the incoming and outgoing protons, respectively. The scattered proton does not leave the beam pipe and can only be detected by using the TOTEM RP detectors, which make a direct measurement of t and ξ (hereafter referred to as ξ_{TOTEM}).

If only CMS information is used, as in Ref. [12], ξ can be estimated only from the energies and longitudinal momenta of the particles measured in CMS:

$$\xi_{CMS}^{\pm} = \frac{\sum_i \left(E^i \pm p_z^i\right)}{\sqrt{s}}, \qquad (2)$$

where the sum is carried out with PF objects. The positive (negative) sign corresponds to the scattered proton moving
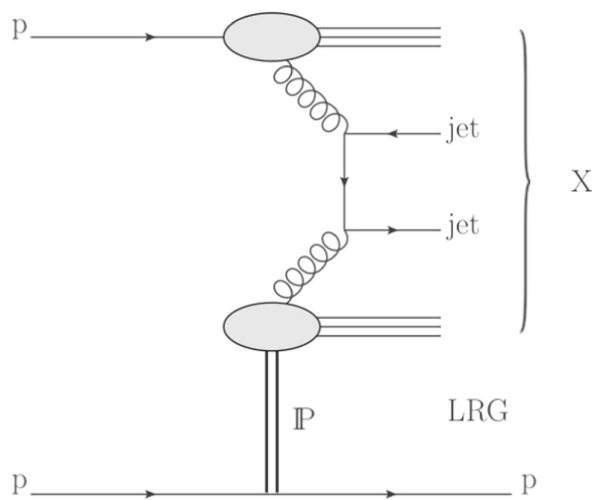
Fig. 1 Schematic diagram of single-diffractive dijet production. The exchange of a virtual object with the vacuum quantum numbers (i.e. a Pomeron) is indicated by the symbol $\mathbb{P}$. The diagram shows an example of the $gg \rightarrow$ dijet hard scattering process; the qq and gq initial states also contribute

towards the positive (negative) z direction. In this case, t cannot be measured.

The combination of the limited CMS pseudorapidity coverage ($|\eta| < 5$) and the detector inefficiency causes ξ_{CMS} to be smaller than ξ_{TOTEM} in general, i.e. $\xi_{\mathrm{CMS}} - \xi_{\mathrm{TOTEM}} \leq 0$. However, the limited detector resolution may cause ξ_{CMS} to be larger than ξ_{TOTEM}.

The momentum fraction of the partons initiating the hard scattering, x^+ and x^-, can be estimated from the energies and longitudinal momenta of the measured jets as:

$$x^{\pm} = \frac{\sum_{\mathrm{jets}} \left(E^{\mathrm{jet}} \pm p_z^{\mathrm{jet}} \right)}{\sqrt{s}}, \qquad (3)$$

where the sum is carried out over the two highest transverse momentum jets in the event, and an additional third jet, if present. The positive (negative) sign corresponds to the incoming proton moving towards the positive (negative) z direction.

Finally, the fraction β of the Pomeron momentum carried by the interacting parton is measured from the values of $x^{\pm}$ and ξ_{TOTEM} as $\beta = x^{\pm}/\xi_{\mathrm{TOTEM}}$.

4 Data samples

The data were collected in July 2012 during a dedicated run with low probability ($\sim$6–10%) of overlapping pp interactions in the same bunch crossing (pileup) and a nonstandard $\beta^* = 90$ m beam optics configuration. These data corre-

spond to an integrated luminosity of $\mathcal{L} = 37.5\,\mathrm{nb}^{-1}$. Events are selected by trigger signals that are delivered simultaneously to the CMS and TOTEM detectors. The first level of the CMS trigger system (L1) is used. The L1 signal is propagated to the TOTEM electronics to enable the simultaneous readout of the CMS and TOTEM subdetectors. The CMS orbit-counter reset signal, delivered to the TOTEM electronics at the start of the run, assures the time synchronisation of the two experiments. The CMS and the TOTEM events are combined offline based on the LHC orbit and bunch numbers.

5 Monte Carlo simulation

The simulation of nondiffractive dijet events is performed with the PYTHIA6 (version 6.422) [30], PYTHIA8 (version 8.153) [31], and HERWIG6 [32] Monte Carlo (MC) event generators. The underlying event is simulated in PYTHIA6 with tune Z2* [33] and in PYTHIA8 with tunes 4C [34], CUETP8M1, and CUETP8S1 [35].

Single-diffractive dijet events are simulated with the PYTHIA8 and POMWIG (version 2.0) [36] generators. Hard diffraction is simulated in PYTHIA8 using an inclusive diffraction model, where both low- and high-mass systems are generated [37]. High-mass diffraction is simulated using a perturbative description. Pomeron parton densities are introduced and the diffractive process is modelled as a proton-Pomeron scattering at a reduced centre-of-mass energy. The default generator settings are used, including that for the proton-Pomeron total cross section. Multiparton interactions (MPI) are included within the proton-Pomeron system to provide cross sections for parton-parton interactions. In this model, the presence of secondary interactions does not lead to a suppression of the visible diffractive cross section.

Additionally, PYTHIA8 implements a model to simulate hard-diffractive events based on a direct application of dPDFs, and a dynamical description of the rapidity gap survival probability in diffractive hadron-hadron interactions [38]. In this model an event is classified as diffractive only when no MPI are generated. We refer to this implementation as the dynamic gap (DG) model. Single-diffractive dijet events using the inclusive diffraction model are simulated with PYTHIA8, tunes 4C and CUETP8M1. The simulation of diffractive dijet events using the DG model is performed with PYTHIA8 version 8.223 [38] with the underlying event tune CUETP8M1. These PYTHIA8 tunes give a fair description of the charged-particle pseudorapidity and p_{T} distributions in a sample with a large fraction of single-diffractive inelastic events [35,39,40].

The POMWIG generator is based on HERWIG6 and implements dPDFs to simulate hard-diffractive processes. The simulation uses dPDFs from a fit to deep inelastic scattering data (H1 fit B [2]). The POMWIG generator uses a next-

to-leading order dPDF fit, whereas PYTHIA8 uses a leading order dPDF fit. When using POMWIG, a constant factor $\langle S^2 \rangle = 7.4\%$ is applied to account for the rapidity gap survival probability leading to the suppression of the diffractive cross section. This value is calculated from the ratio of the measured diffractive cross section and the prediction from POMWIG, as described in Sect. 8.2. Both Pomeron and Reggeon exchange contributions are generated. Reggeon exchange is not simulated in PYTHIA8.

To improve the description of the data by the MC samples, correction factors are applied event-by-event as a function of β, by a reweighting procedure. The correction modifies the event distribution as a function of β by up to 40%, and the $\log_{10} x$ and ξ distributions by as much as 30% and 8%, respectively. The correction has a negligible effect on the t distribution.

The generated events are processed through the simulation of the CMS detector, based on GEANT4 [41], and reconstructed in the same manner as the data. The acceptance and resolution of the TOTEM RP detectors are parametrised as a function of the proton kinematics, as discussed below. All samples are simulated without pileup.

5.1 Roman pot detectors acceptance and resolution

The proton path from the IP to the TOTEM RPs is calculated using a parametrisation of the LHC optics [27]. To obtain a realistic simulation of the scattered proton, the following procedure is used:

– *Proton transport:* The simulation of the RP detectors acceptance is parametrised in terms of the vertex position, the proton scattering angles at the vertex θ_x^* and θ_y^*, and ξ. The incident beam energy spread and beam divergence are also simulated [29].
– *Reconstruction of t and ξ:* The detector-level distributions of t and ξ are obtained from the scattering angles θ_x^* and θ_y^*, where the correlation between the ξ and θ_x^* uncertainties is taken into account [26]. The generated values of θ_x^* and θ_y^* are spread by $25\,\mu$rad and $2.4\,\mu$rad, respectively. These values include the effects of detector resolution, as well as those of the beam optics and the beam divergence.
– *Proton reconstruction inefficiency:* The track reconstruction in the RPs may fail for several reasons: inefficiency of the silicon sensors, interaction of the proton with the RP mechanics, or the simultaneous presence of a beam halo particle or a proton from a pileup interaction. The silicon strips of the detectors in an RP are oriented in two orthogonal directions; this allows for good rejection of inclined background tracks, but makes it very difficult to reconstruct more than one track almost parallel to the beam direction [26]. These uncorrelated inefficiencies are

evaluated from elastic scattering data [29], and amount to ∼6%. To correct for this, an extra normalisation factor is applied, obtained separately for protons traversing the RPs on either side of the IP.

6 Event selection

Dijet events are selected online by requiring at least two jets with $p_T > 20$ GeV [42]. The efficiency of this trigger selection is estimated with a sample of minimum bias events, i.e. events collected with a loose trigger intended to select inelastic collisions with as little bias as possible, and containing a leading jet with p_T, as reconstructed offline, of at least 40 GeV. The fraction of dijet events accepted by the trigger is calculated as a function of the subleading jet p_T. The efficiency is above 94% for $p_T > 40$ GeV.

The offline selection requires at least two jets with $p_T > 40$ GeV and $|\eta| < 4.4$. Jets are reconstructed from PF objects with the anti-k_T algorithm with a distance parameter $R = 0.5$. The reconstructed jet energy is corrected with the procedure described in Ref. [22]. The parton momentum fractions x^+ and x^- are reconstructed using Eq. (3) from the two highest transverse momentum jets and an additional third jet, if present. The latter is selected with $p_T > 20$ GeV. In addition, the selection requires at least one reconstructed primary interaction vertex and at least one reconstructed proton track in the RP stations. The fit of the reconstructed vertex is required to have more than four degrees of freedom.

Events with protons in the RP stations on both sides are rejected if their kinematics are consistent with those of elastic scattering. Elastic scattering events, which are present in the data sample because of pileup, are identified by the presence of two proton tracks in opposite directions, in a diagonal configuration: the protons traverse the two top RPs in sector 45 and the two bottom RPs in sector 56, or vice versa. The horizontal and vertical scattering angles are required to match within the measured resolutions. These requirements are similar to those described in Ref. [29].

To avoid detector edges with rapidly varying efficiency or acceptance, as well as regions dominated by secondary particles produced by aperture limitations in the beamline upstream of the RPs, proton track candidates are selected if the corresponding hit coordinates on the RP stations satisfy the following fiducial requirements: $0 < x < 7$ mm and $8.4 < |y| < 27$ mm, where x and y indicate the horizontal and vertical coordinates of the hit with respect to the beam.

To suppress background from secondary particles and pileup in the RPs, the reconstructed proton track is selected if it is associated to one track element in both top or both bottom RPs on a given side. The kinematic requirements $0.03 < |t| < 1.0$ GeV^2 and $0 < \xi_{\text{TOTEM}} < 0.1$ are then applied.

For signal events, one expects ξ_{CMS} to be smaller than ξ_{TOTEM}, i.e. $\xi_{CMS} - \xi_{TOTEM} \leq 0$ (as discussed in Sect. 3). This selection is imposed to suppress the contribution of pileup and beam halo events, in which the proton is uncorrelated with the hadronic final state X measured in the CMS detector. Roughly 6% of signal events are rejected by this requirement, as estimated from a simulation of single-diffractive dijet production.

Table 1 shows the number of events passing each selection. The number of events with the proton detected in the RPs in sector 45 (56) after all the selections is 368 (420).

A difference in the yields for events with a proton in sector 45 and 56 could notably arise from different background contributions, which is discussed in Sect. 7. Both an imperfect knowledge of the optical functions, especially the horizontal dispersion, discussed in Sect. 8.1, and statistical fluctuations of the two mostly independent event samples contribute to the difference.

7 Background

The main background is due to the overlap of a pp collision in the CMS detector and an additional track in the RP stations, originating from either a beam halo particle or an outgoing proton from a pileup interaction.

Pileup and beam halo events are not simulated, but they are present in the data. To estimate the pileup and beam halo contribution in the data, a zero bias sample consisting of events from randomly selected, nonempty LHC bunch crossings is used. Events with a proton measured in the RP stations and with any number of reconstructed vertices are selected from the zero bias data set. Such events are denoted by ZB in the following.

The RP information from events in the zero bias sample is added to diffractive and nondiffractive events generated with POMWIG and PYTHIA6, respectively. The mixture of MC and ZB events simulates data events in the presence of pileup and beam halo.

The POMWIG sample is normalised assuming a rapidity gap survival probability factor of 7.4%, as discussed in Sect. 5. The MC and ZB event mixture is then passed through the selection procedure illustrated in Sect. 6, except for the requirement $\xi_{CMS} - \xi_{TOTEM} \leq 0$, which is not applied.

Such mixed events with a proton in the RPs are considered as signal if the proton originates from the MC simulated sample, or as background if it originates from the ZB sample. If an event has a proton from both the MC sample and the ZB sample, the proton with smaller ξ is chosen. However, the probability of such a combination is small and none of these events pass all the selections. Figure 2 shows the distribution of $\xi_{CMS} - \xi_{TOTEM}$ for the data compared to the MC+ZB event mixture. The requirement $\xi_{CMS} - \xi_{TOTEM} \leq 0$ selects signal

events and rejects the kinematically forbidden region populated by the MC+ZB background events (filled histogram). The background distribution is normalised to the data in the $\xi_{CMS} - \xi_{TOTEM}$ region from 0.048 to 0.4, which is dominated by background events.

The background is estimated separately for events with a proton traversing the two top (top-top) or the two bottom (bottom-bottom) RPs on each side. The top-top and bottom-bottom distributions are similar. Figure 2 shows the sum of the two contributions.

The background contribution for events with a proton detected in sector 56 (right panel of Fig. 2) is larger than that for events with a proton detected in sector 45 (left panel of Fig. 2). The remaining contamination of background in the signal region is estimated to be 15.7% for events in which the proton is detected in sector 45 and 16.8% for those in which the proton is detected in sector 56.

Figure 3 shows the distribution of ξ_{TOTEM} for the data and the MC+ZB sample, before and after the $\xi_{CMS} - \xi_{TOTEM} \leq 0$ requirement, as well as the distribution of t, after the $\xi_{CMS} - \xi_{TOTEM} \leq 0$ selection. The sum of the top-top and bottom-bottom combinations is used. The data and the MC+ZB sample are in good agreement.

An alternative method, used at HERA [4], takes two events randomly chosen from the data sample. First, ξ_{CMS} is sampled from events that have passed the dijet selection; ξ_{TOTEM} is then taken from events with $\xi_{CMS} > 0.12$ that have passed the event selection described in Sect. 6, except for the $\xi_{CMS} - \xi_{TOTEM}$ requirement, to select proton tracks considered to be mostly from background. These two values are used to plot the $\xi_{CMS} - \xi_{TOTEM}$ distribution, which is normalised to the data in a region dominated by background. The remaining contamination in the signal region is ∼19% both for events with a proton detected in sector 45 and for those with a proton in sector 56. The ZB method is used in this analysis. Half the difference between the results of the two methods is taken as an estimate of the systematic uncertainty of the background subtraction procedure.

8 Results

In this section the measurements of the differential cross sections $d\sigma/dt$, $d\sigma/d\xi$, and the ratio $R(x)$ of the single-diffractive ($\sigma_{jj}^{pX}(x)$) to inclusive dijet cross sections ($\sigma_{jj}(x)$) are presented. The ratio $R(x)$, normalised per unit of ξ, is defined by:

$$R(x) = \frac{\sigma_{jj}^{pX}(x)/\Delta\xi}{\sigma_{jj}(x)}, \tag{4}$$

where $\Delta\xi = 0.1$.

Table 1 Number of events after each selection

Selection	Sector 45	Sector 56
At least 2 jets ($p_T > 40$ GeV, $|\eta| < 4.4$)	427689	
Elastic scattering veto	405112	
Reconstructed proton	9530	
RP and fiducial region	2137	3033
$0.03 < |t| < 1.0$ GeV^2, $0 < \xi_{\text{TOTEM}} < 0.1$	1393	1806
$\xi_{\text{CMS}} - \xi_{\text{TOTEM}} \leq 0$	368	420
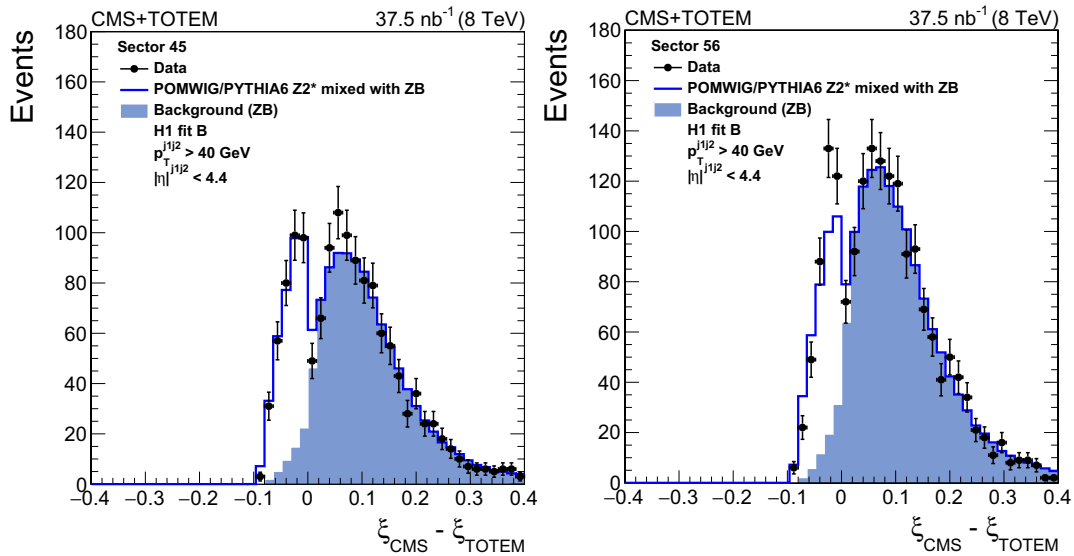
Fig. 2 Distribution of $\xi_{\text{CMS}} - \xi_{\text{TOTEM}}$ for events with a reconstructed proton in sector 45 (left) and sector 56 (right). The data are indicated by solid circles. The blue histogram is the mixture of POMWIG or PYTHIA6 and zero bias (ZB) data events described in the text. An event with a proton measured in the RPs contributes to the open histogram (signal) if the proton originates from the MC sample, or to the filled histogram (background) if it originates from the ZB sample

The cross sections are calculated in the kinematic region $\xi < 0.1$, $0.03 < |t| < 1$ GeV^2, with at least two jets at a stable-particle level with $p_T > 40$ GeV and $|\eta| < 4.4$. The ratio $R(x)$ is calculated for x values in the region $-2.9 \leq \log_{10} x \leq -1.6$. In the following, the estimated background is subtracted from the number of single-diffractive dijet candidates following the procedure described in the previous section.

The differential cross sections for dijet production in bins of t and ξ are evaluated as:

$$\frac{\mathrm{d}\sigma_{jj}^{pX}}{\mathrm{d}t} = \mathcal{U}\left\{\frac{N_{jj}^{pX}}{\mathcal{L}A_{\text{CMS–TOTEM}}\Delta t}\right\},$$

$$\frac{\mathrm{d}\sigma_{jj}^{pX}}{\mathrm{d}\xi} = \mathcal{U}\left\{\frac{N_{jj}^{pX}}{\mathcal{L}A_{\text{CMS–TOTEM}}\Delta\xi}\right\}, \tag{5}$$

where N_{jj}^{pX} is the measured number of single-diffractive dijet candidates per bin of the distribution after subtracting the estimated background; Δt and $\Delta\xi$ are the bin widths, and $\mathcal{L}$ is the integrated luminosity. The factors $A_{\text{CMS–TOTEM}}$ indicate the acceptance of CMS and TOTEM for single-diffractive dijet events. Unfolding corrections, represented by the symbol $\mathcal{U}$ in Eq. (5), are applied to account for the finite resolution of the reconstructed variables used in the analysis. They are evaluated with POMWIG, PYTHIA8 4C and PYTHIA8 CUETP8M1. The results presented are the average of those obtained with the different unfolding corrections. The measured cross sections are obtained by unfolding the data using the D'Agostini method with early stopping [43]. In this method the regularisation parameter is the number of iterations used, which is optimised to obtain a relative χ^2 variation between iterations lower than 5%.
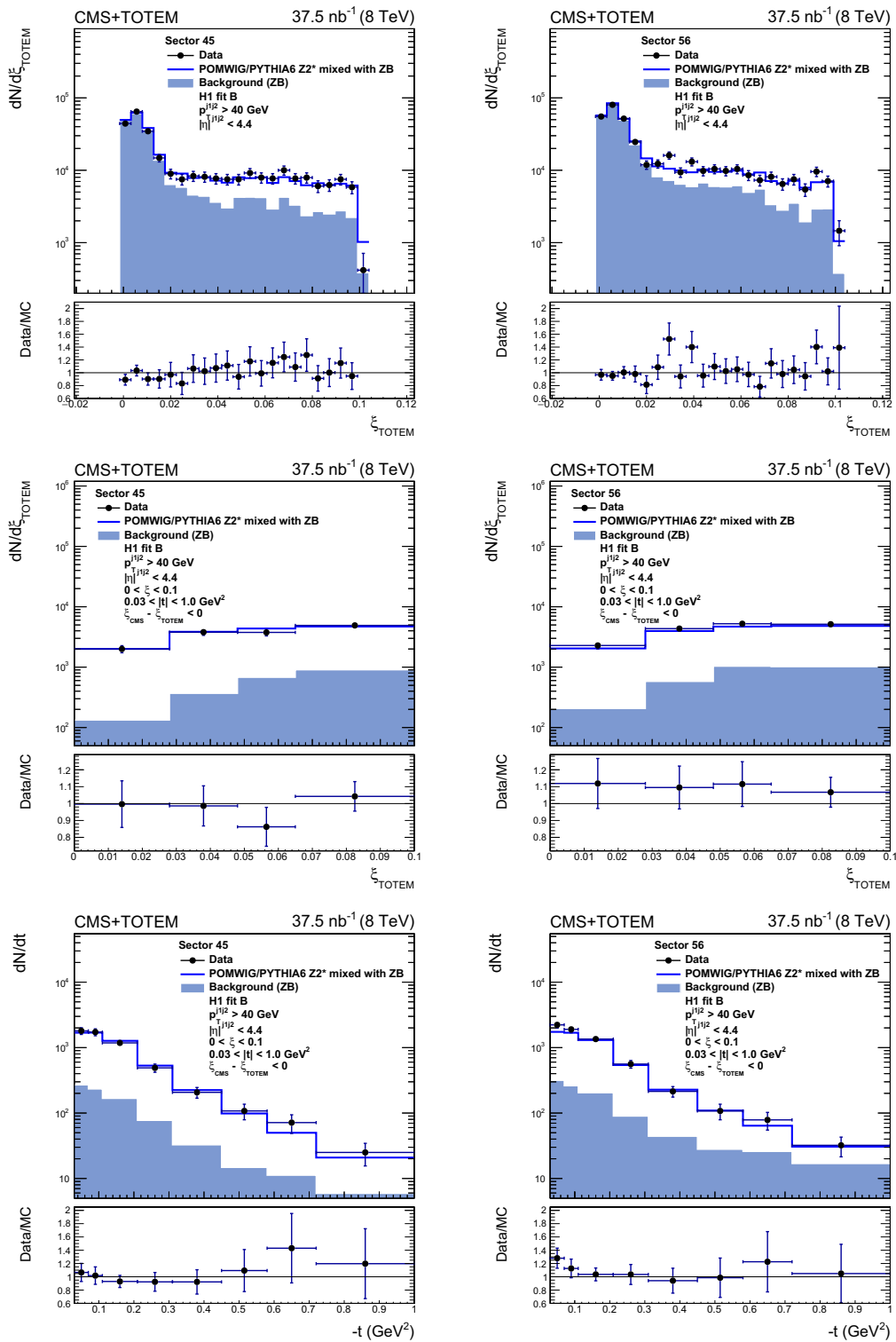
Fig. 3 Distribution of ξ_{TOTEM} before (upper) and after (middle) the $\xi_{CMS} - \xi_{TOTEM}$ requirement and distribution of t after the $\xi_{CMS} - \xi_{TOTEM}$ requirement (lower) for events in which the proton is detected in sector 45 (left) and sector 56 (right). The data are indicated by solid circles. The blue histogram is the mixture of POMWIG or PYTHIA6 and zero bias

(ZB) data events described in the text. An event with the proton measured in the RPs contributes to the open histogram (signal) if the proton originates from the MC sample, or to the filled histogram (background) if it originates from the ZB sample

The ratio $R(x)$ of the single-diffractive to inclusive dijet cross sections is evaluated as a function of x as:

$$R(x) = \frac{\sigma_{jj}^{pX}(x)/\Delta\xi}{\sigma_{jj}(x)} = \frac{\mathcal{U}\left\{N_{jj}^{pX}/A_{CMS-TOTEM}\right\}/\Delta\xi}{\mathcal{U}\left\{N_{jj}/A_{CMS}\right\}}, \quad (6)$$

where N_{jj}^{pX} is the number of single-diffractive dijet candidates with $\xi_{TOTEM} < 0.1$, and N_{jj} is the total number of dijet events without the requirement of a proton detected in the RPs. This number is dominated by the nondiffractive contribution. The symbol $A_{CMS-TOTEM}$ indicates the acceptance of CMS and TOTEM for single-diffractive dijet events, evaluated with POMWIG, PYTHIA8 4C and PYTHIA8 CUETP8M1; A_{CMS} is the acceptance for nondiffractive dijet production ($p_T > 40\,\text{GeV}$, $|\eta| < 4.4$), evaluated with PYTHIA6, PYTHIA8 4C, PYTHIA8 CUETP8M1, PYTHIA8 CUETP8S1, and HERWIG6. The acceptance includes unfolding corrections to the data with the D'Agostini method with early stopping, denoted by the symbol $\mathcal{U}$ in Eq. (6).

8.1 Systematic uncertainties

The systematic uncertainties are estimated by varying the selections and modifying the analysis procedure, as discussed in this section. Tables 2 and 3 summarise the main systematic uncertainties of the single-diffractive cross section and the ratio of the single-diffractive and inclusive dijet cross sections, respectively, presented in Sects. 8.2 and 8.3.

- *Trigger efficiency:* The trigger efficiency is calculated as a function of the subleading jet p_T using a fit to the data. The sensitivity to the trigger efficiency determination is estimated by varying the fit parameters within their uncertainties. This variation corresponds to a trigger efficiency that increases or decreases by roughly 2% at jet $p_T = 40\,\text{GeV}$ and less than 1% at $p_T = 50\,\text{GeV}$.
- *Calorimeter energy scale:* The reconstruction of ξ_{CMS} is affected by the uncertainty in the calorimeter energy scale and is dominated by the HF contribution. This uncertainty is estimated by changing the energy of the PF candidates by $\pm 10\%$ [12,44].
- *Jet energy scale and resolution:* The energy of the reconstructed jets is varied according to the jet energy scale uncertainty following the procedure described in Ref. [22]. The systematic uncertainty in the jet energy resolution is estimated by varying the scale factors applied to the MC, as a function of pseudorapidity. The uncertainties obtained from the jet energy scale and resolution are added in quadrature. The effect of the jet energy resolution uncertainty amounts to less than 1% of the measured cross section.

- *Background:* Half the difference between the results of the ZB and HERA methods used to estimate the background, described in Sect. 7, is an estimate of the effect of the systematic uncertainty of the background.
- *RP acceptance:* The sensitivity to the size of the fiducial region for the impact position of the proton in the RPs is estimated by modifying its vertical boundaries by $200\,\mu\text{m}$ and by reducing the horizontal requirement by 1 mm, to $0 < x < 6$ mm. Half the difference of the results thus obtained and the nominal ones is used as a systematic uncertainty. The uncertainties obtained when modifying the vertical and horizontal boundaries are added in quadrature.
- *Resolution:* The reconstructed variables t and ξ are calculated by applying two methods: either directly, with a resolution function depending on each of these variables, or indirectly from the scattering angles θ_x^* and θ_y^*. Half the difference between the results using the two methods is taken as a systematic uncertainty.
- *Horizontal dispersion:* The reconstructed ξ value depends on the optical functions describing the transport of the protons from the interaction vertex to the RP stations, and specifically the horizontal dispersion. This uncertainty is calculated by scaling the value of ξ by $\pm 10\%$. This value corresponds to a conservative limit of the possible horizontal dispersion variation with respect to the nominal optics.
- *t-slope:* The sensitivity to the modelling of the exponential t-slope is quantified by replacing its value in POMWIG by that measured in the data. Half the difference between the results thus found and the nominal results is used as an estimate of the uncertainty.
- *β-reweighting:* Half the difference of the results with and without the reweighting as a function of β in POMWIG (as discussed in Sect. 5) is included in the systematic uncertainty. The effect amounts to less than 1% of the single-diffractive cross section and less than about 6% of the single-diffractive to inclusive dijet cross section ratio versus x.
- *Acceptance and unfolding:* Half the maximum difference between the single-diffractive cross section results found by unfolding with POMWIG, PYTHIA8 4C, and PYTHIA8 CUETP8M1 is taken as a further component of the systematic uncertainty. Likewise for the results obtained with PYTHIA6 Z2*, PYTHIA8 4C, PYTHIA8 CUETP8M1 and PYTHIA8 CUETP8S1 for the inclusive dijet cross section.
- *Unfolding regularisation:* The regularisation parameter used in the unfolding, given by the number of iterations in the D'Agostini method used in this analysis, is optimised by calculating the relative χ^2 variation between iterations. The value is chosen such that the χ^2 variation is below 5%. The number of iterations when the rela-

tive variation of χ^2 is below 2% is also used and half the difference with respect to the nominal is taken as a systematic uncertainty.

– *Unfolding bias:* A simulated sample, including all detector effects, is unfolded with a different model. The difference between the corrected results thus obtained and those at the particle level is an estimate of the bias introduced by the unfolding procedure. Half the maximum difference obtained when repeating the procedure with all generator combinations is a measure of the systematic uncertainty related to the unfolding.

– *Integrated luminosity:* The uncertainty in the integrated luminosity is 4%, measured using a dedicated sample collected by TOTEM during the same data taking period [29].

The total systematic uncertainty is calculated as the quadratic sum of the individual contributions. The uncertainties in the jet energy scale and horizontal dispersion are the dominant contributions overall.

8.2 Extraction of the cross section as a function of t and ξ

Figure 4 shows the differential cross section as a function of t and ξ, integrated over the conjugate variable. The results from events in which the proton is detected on either side of the IP are averaged.

The data are compared to POMWIG, PYTHIA8 4C, PYTHIA8 CUETP8M1, and PYTHIA8 DG. The POMWIG prediction is shown for two values of the suppression of the diffractive cross section, i.e. the rapidity gap survival probability, represented by $\langle S^2 \rangle$. When $\langle S^2 \rangle = 1$, no correction is applied. The resulting cross sections are higher than the data by roughly an order of magnitude, in agreement with the Tevatron results [9–11]. The POMWIG prediction is also shown with the correction $\langle S^2 \rangle = 7.4\%$, calculated from the ratio of the measured diffractive cross section and the MC prediction, as discussed below. After this correction, POMWIG gives a good description of the data. The POMWIG prediction is shown in Fig. 4 as the sum of the Pomeron (p$\mathbb{P}$), Reggeon (p$\mathbb{R}$) and Pomeron-Pomeron ($\mathbb{P}\mathbb{P}$) exchange contributions, while PYTHIA8 includes only the Pomeron (p$\mathbb{P}$) contribution. PYTHIA8 4C and PYTHIA8 CUETP8M1 predict cross sections higher than the data by up to a factor of two. The PYTHIA8 DG model shows overall a good agreement with the data. No correction is applied to the normalisation of the PYTHIA8 samples. The PYTHIA8 DG model is the only calculation that predicts the cross section normalisation without an additional correction.

The ratio between the data and the POMWIG predictions is shown in the bottom of the left and right panels of Fig. 4. No correction is applied for the rapidity gap survival probability ($\langle S^2 \rangle = 1$). Within the uncertainties, no significant dependence on t and ξ is observed.

The value of the cross section for single-diffractive dijet production, measured in the kinematic region $p_T > 40$ GeV, $|\eta| < 4.4$, $\xi < 0.1$ and $0.03 < |t| < 1$ GeV^2, is:

$$\sigma_{jj}^{pX} = 21.7 \pm 0.9\,(\text{stat})\,{}^{+3.0}_{-3.3}\,(\text{syst}) \pm 0.9\,(\text{lumi})\,\text{nb}. \qquad (7)$$

Table 2 summarises the main systematic uncertainties of the measured cross section. The cross section is calculated independently for events in which the proton scatters towards the positive and negative z directions, namely the processes pp $\rightarrow$ pX and pp $\rightarrow$ Xp, and the results are averaged. They are compatible within the uncertainties. The PYTHIA8 DG model predicts in the same kinematic region a cross section of 23.7 nb, consistent with the measurement.

The differential cross section as a function of t is well described by an exponential function for $|t|$ values up to about 0.4 GeV^2. A fit is performed with the function $d\sigma/dt \propto \exp(-b|t|)$ for t values in the range $0.03 < |t| < 0.45$ GeV^2.

The resulting exponential slope is:

$$b = 6.5 \pm 0.6\,(\text{stat})\,{}^{+1.0}_{-0.8}\,(\text{syst})\,\text{GeV}^{-2}, \qquad (8)$$

where the systematic uncertainties include the contributions discussed in Sect. 8.1. The results for the exponential slope of the cross section calculated independently for events in which the proton scatters towards the positive and negative z directions are compatible within the uncertainties.

The parametrisation obtained from the fit is shown in Fig. 4. In the fit range ($0.03 < |t| < 0.45$ GeV^2), the horizontal position of the data points is calculated as the value for which the parametrised function equals its average over the bin width. The data points in the larger-$|t|$ region outside the fit range ($|t| > 0.45$ GeV^2) are shown at the centre of the bins.

The slope measured by CDF is $b \approx 5$–6 GeV^{-2} for $|t| \lesssim 0.5$ GeV^2 [10]. In the larger-$|t|$ region, the CDF data exhibit a smaller slope that becomes approximately independent of t for $|t| \gtrsim 2$ GeV^2.

The present measurement of the slope is consistent with that by CDF at small-$|t|$. The data do not conclusively indicate a flattening of the t distribution at larger-$|t|$.

An estimate of the rapidity gap survival probability can be obtained from the ratio of the measured cross section in Eq. (7) and that predicted by POMWIG with $\langle S^2 \rangle = 1$. Alternatively, the PYTHIA8 hard-diffraction model can be used if the DG suppression framework is not applied. The two results are consistent.

The overall suppression factor obtained with respect to the POMWIG cross section is $\langle S^2 \rangle = 7.4\,{}^{+1.0}_{-1.1}\%$, where the statistical and systematic uncertainties are added in quadrature.
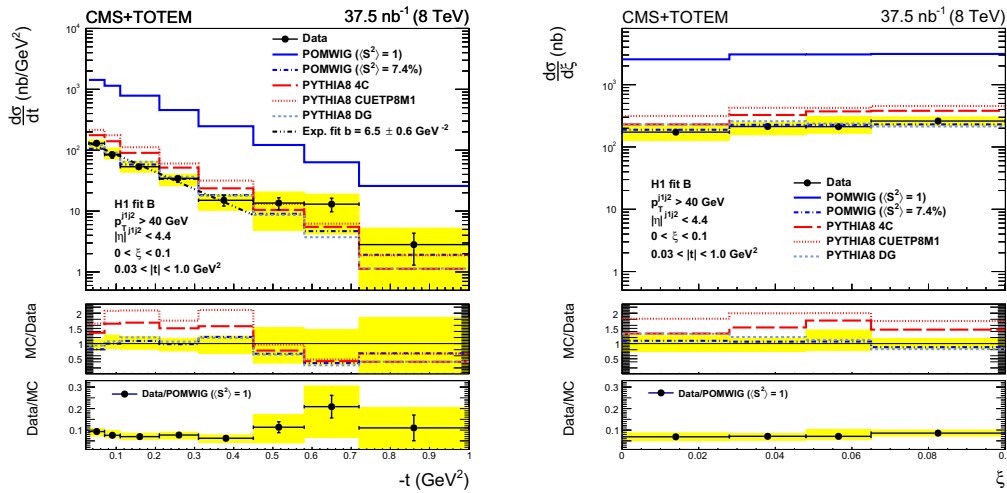
Fig. 4 Differential cross section as a function of t (left) and as a function of ξ (right) for single-diffractive dijet production, compared to the predictions from POMWIG, PYTHIA8 4C, PYTHIA8 CUETP8M1, and PYTHIA8 DG. The POMWIG prediction is shown with no correction for the rapidity gap survival probability ($\langle S^2 \rangle = 1$) and with a correction of $\langle S^2 \rangle = 7.4\%$. The vertical bars indicate the statistical uncertainties and the yellow band indicates the total systematic uncertainty. The average of the results for events in which the proton is detected on either side of the interaction point is shown. The ratio between the data and the POMWIG prediction, when no correction for the rapidity gap survival probability is applied, is shown in the bottom

Table 2 Individual contributions to the systematic uncertainties in the measurement of the single-diffractive dijet production cross section in the kinematic region $p_T > 40$ GeV, $|\eta| < 4.4$, $\xi < 0.1$, and $0.03 < |t| < 1$ GeV^2. The second column indicates the relative uncertainties in the integrated cross section. The third and fourth columns represent the minimum and maximum relative uncertainties in the differential cross sections in bins of t and ξ, respectively. The minimum relative uncertainty is not shown when it is below 1%. The total uncertainty is the quadratic sum of the individual contributions. The uncertainty of the integrated luminosity is not shown

Uncertainty source	Relative uncertainty		
	σ_{jj}^{pX}	$d\sigma/dt$	$d\sigma/d\xi$
Trigger efficiency	$\pm 2\%$	1–2%	< 2.4%
Calorimeter energy scale	$+ 1/- 2\%$	< 7%	< 7%
Jet energy scale and resolution	$+ 9/- 8\%$	3–32%	7–16%
Background	$\pm 3\%$	2–27%	< 8%
RP acceptance	< 1%	< 21%	< 2%
Resolution	$\pm 2\%$	2–30%	< 8%
Horizontal dispersion	$+ 9/- 12\%$	8–71%	8–41%
t-slope	< 1%	< 16%	< 1.3%
β-reweighting	< 1%	< 1%	< 1%
Acceptance and unfolding	$\pm 2\%$	2–50%	5–12%
Unfolding bias	$\pm 3\%$	2–50%	5–11%
Unfolding regularization	—	< 8%	< 1%
Total	$+ 14/- 15\%$		

A similar result is obtained when the PYTHIA8 unsuppressed cross section is used as reference value.

The H1 fit B dPDFs used in this analysis include the contribution from proton dissociation in ep collisions. They are extracted from the process ep $\rightarrow$ eXY, where Y can be a proton or a low-mass excitation with $M_Y < 1.6$ GeV [2]. The results found when the proton is detected are consistent, apart from a different overall normalisation. The ratio of the cross sections is $\sigma(M_Y < 1.6 \, \text{GeV})/\sigma(M_Y = M_p) = 1.23 \pm 0.03 \, (\text{stat}) \pm 0.16 \, (\text{syst})$ [2,3]. No dependence on β, Q^2, or ξ is observed. To account for the different normalisation, the ratio is used to correct $\langle S^2 \rangle$; this yields $\langle S^2 \rangle = (9 \pm 2)\%$ when the POMWIG cross section is taken as the reference value. A similar result is obtained with PYTHIA8.
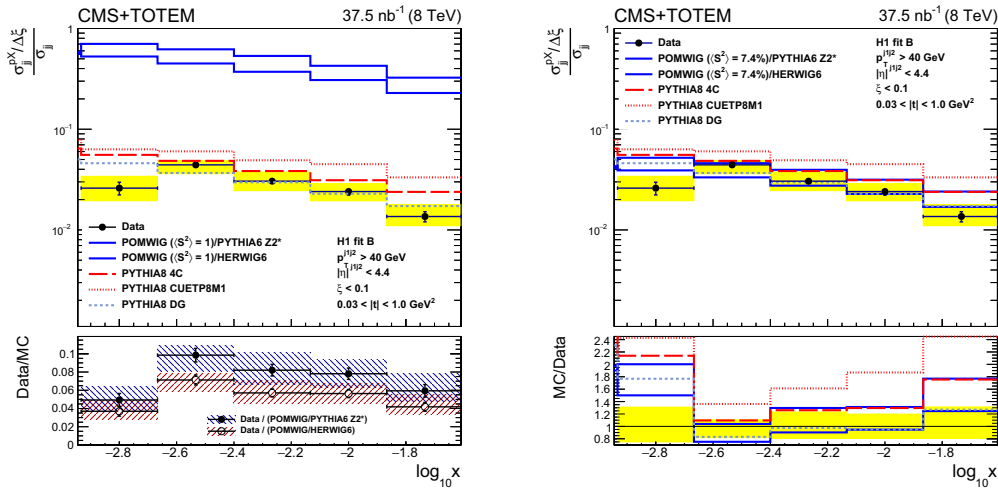
Fig. 5 Ratio per unit of ξ of the single-diffractive and inclusive dijet cross sections in the region given by $\xi < 0.1$ and $0.03 < |t| < 1\,\text{GeV}^2$, compared to the predictions from the different models for the ratio between the single-diffractive and nondiffractive cross sections. The POMWIG prediction is shown with no correction for the rapidity gap survival probability ($\langle S^2 \rangle = 1$) (left) and with a correction of $\langle S^2 \rangle = 7.4\%$ (right). The vertical bars indicate the statistical uncertainties and the yel-

low band indicates the total systematic uncertainty. The average of the results for events in which the proton is detected on either side of the interaction point is shown. The ratio between the data and the POMWIG prediction using PYTHIA6 or HERWIG6 as the nondiffractive contribution, when no correction for the rapidity gap survival probability is applied, is shown in the bottom of the left panel

8.3 Extraction of the ratio of the single-diffractive to inclusive dijet yields

Figure 5 shows the ratio $R(x)$ in the kinematic region $p_\text{T} > 40\,\text{GeV}$, $|\eta| < 4.4$, $\xi < 0.1$, $0.03 < |t| < 1\,\text{GeV}^2$ and $-2.9 \leq \log_{10} x \leq -1.6$. The average of the results for events in which the proton is detected on either side of the IP is shown. The yellow band represents the total systematic uncertainty (cf. Sect. 8.1). The data are compared to the ratio of the single-diffractive and nondiffractive dijet cross sections from different models. The single-diffractive contribution is simulated with POMWIG, PYTHIA8 4C, PYTHIA8 CUETP8M1, and PYTHIA8 DG. The nondiffractive contribution is simulated with PYTHIA6 and HERWIG6 if POMWIG is used for the diffractive contribution. When using PYTHIA8 the diffractive and nondiffractive contributions are simulated with the same underlying event tune. When no correction for the rapidity gap survival probability is applied ($\langle S^2 \rangle = 1$), POMWIG gives a ratio higher by roughly an order of magnitude, consistent with the results discussed in Sect. 8.2. The suppression seen in the data with respect to the simulation is not substantially different when using PYTHIA6 or HERWIG6 for the nondiffractive contribution. POMWIG with a correction of $\langle S^2 \rangle = 7.4\%$ gives, as expected, a good description of the data. When HERWIG6 is used for the nondiffractive contribution the agreement is worse, especially in the lower- and higher-x regions. The agreement for PYTHIA8 4C is fair in

the intermediate x region, but worse at low- and high-x. The agreement is worse for PYTHIA8 CUETP8M1, with values of the ratio higher than those in the data by up to a factor of two. The PYTHIA8 DG predictions agree well with the data, though the agreement is worse in the low-x region. No correction is applied to the PYTHIA8 normalisation. In the lowest-x bin, the ratio in the data is below the predictions. The observed discrepancy is not significant for the predictions that agree well overall with the data elsewhere, taking into account the systematic and statistical uncertainties.

The measured value of the ratio, normalised per unit of ξ, in the full kinematic region defined above is:

$$R = \left(\sigma_{\text{jj}}^{\text{pX}} / \Delta\xi \right) / \sigma_{\text{jj}} = 0.025 \pm 0.001\,(\text{stat}) \pm 0.003\,(\text{syst}).$$
(9)

Table 3 summarises the main contributions to the systematic uncertainty of the ratio. The uncertainty of the jet energy scale is considerably smaller than in the case of the single-diffractive cross section.

Figure 6 shows the comparison between the results of Fig. 5 and those from CDF [10]. The CDF results are shown for jets with Q^2 of roughly $100\,\text{GeV}^2$ and pseudorapidity $|\eta| < 2.5$, with $0.03 < \xi < 0.09$. In this case Q^2 is defined, per event, as the mean transverse energy of the two leading jets squared. CDF measures the ratio for Q^2 values up to $10^4\,\text{GeV}^2$. A relatively small dependence on Q^2 is observed.

Table 3 Individual contributions to the systematic uncertainty in the measurement of the single-diffractive to inclusive dijet yields ratio in the kinematic region $p_T > 40$ GeV, $|\eta| < 4.4$, $\xi < 0.1$, $0.03 < |t| < 1$ GeV^2, and $-2.9 \leq \log_{10} x \leq -1.6$. The second and third columns represent the relative uncertainties in the ratio in the full kinematic region and in bins of $\log_{10} x$, respectively. The minimum relative uncertainty is not shown when it is below 1%. The total uncertainty is the quadratic sum of the individual contributions

Uncertainty source	Relative uncertainty	
	R	$R(x)$
Trigger efficiency	Negligible	2–3%
Calorimeter energy scale	$+1/-2\%$	< 7%
Jet energy scale and resolution	±2%	1–10%
Background	±1%	1–17%
RP acceptance	< 1%	< 4%
Resolution	±2%	< 4%
Horizontal dispersion	$+9/-11\%$	11–23%
t-slope	< 1%	< 3%
β-reweighting	±1 %	< 6%
Acceptance and unfolding	±2 %	3–11%
Unfolding bias	±3%	3–14%
Unfolding regularization	—	< 11%
Total	$+10/-13\%$	

Fig. 6 Ratio per unit of ξ of the single-diffractive and inclusive dijet cross sections in the kinematic region given by $\xi < 0.1$ and $0.03 < |t| < 1$ GeV^2. The vertical bars indicate the statistical uncertainties and the yellow band indicates the total systematic uncertainty. The red squares represent the results obtained by CDF at $\sqrt{s} = 1.96$ TeV for jets with $Q^2 \approx 100$ GeV^2 and $|\eta| < 2.5$, with $0.03 < \xi < 0.09$

The present data are lower than the CDF results. A decrease of the ratio of diffractive to inclusive cross sections with centre-of-mass energy has also been observed by CDF by comparing data at 630 and 1800 GeV [11].

9 Summary

The differential cross section for single-diffractive dijet production in proton–proton (pp) collisions at $\sqrt{s} = 8$ TeV has been measured as a function of the proton fractional momentum loss ξ and the squared four momentum transfer t, using the CMS and TOTEM detectors. The data, corresponding to an integrated luminosity of 37.5 nb^{-1}, were collected using a nonstandard optics configuration with $\beta^* = 90$ m. The processes considered are pp $\rightarrow$ pX or pp $\rightarrow$ Xp, with X including a system of two jets, in the kinematic region $\xi < 0.1$ and $0.03 < |t| < 1.0$ GeV^2. The two jets have transverse momentum $p_T > 40$ GeV and pseudorapidity $|\eta| < 4.4$. The integrated cross section in this kinematic region is $\sigma_{jj}^{pX} = 21.7 \pm 0.9$ (stat) $^{+3.0}_{-3.3}$ (syst) ± 0.9 (lumi) nb; it is the average of the cross sections when the proton scatters to either side of the interaction point. The exponential slope of the cross section as a function of t is $b = 6.5 \pm 0.6$ (stat) $^{+1.0}_{-0.8}$ (syst) GeV^{-2}. This is the first measurement of hard diffraction with a measured proton at the LHC.

The data are compared with the predictions of different models. After applying a normalisation shift ascribed to the rapidity gap survival probability, POMWIG agrees well with the data. The PYTHIA8 dynamic gap model describes the data well, both in shape and normalisation. In this model the effects of the rapidity gap survival probability are simulated within the framework of multiparton interactions. The PYTHIA8 dynamic gap model is the only calculation that predicts the cross section normalisation without an additional correction.

The ratios of the measured single-diffractive cross section to those predicted by POMWIG and PYTHIA8 give estimates of the rapidity gap survival probability. After accounting for the correction of the dPDF normalisation due to proton dissociation, the value of $\langle S^2 \rangle$ is (9 ± 2) % when using POMWIG as the reference cross section value, with a similar result when PYTHIA8 is used.

The ratio of the single-diffractive to inclusive dijet cross section has been measured as a function of the parton momentum fraction x. The ratio is lower than that observed at CDF at a smaller centre-of-mass energy. In the region $p_T > 40$ GeV, $|\eta| < 4.4$, $\xi < 0.1$, $0.03 < |t| < 1.0$ GeV^2, and $-2.9 \leq \log_{10} x \leq -1.6$, the ratio, normalised per unit ξ, is $R = (\sigma_{jj}^{pX}/\Delta\xi)/\sigma_{jj} = 0.025 \pm 0.001$ (stat) ± 0.003 (syst).

Data Availability Statement This manuscript has no associated data or the data will not be deposited. [Authors' comment: Release and preservation of data used by the CMS Collaboration as the basis for publications is guided by the CMS policy as written in its document "CMS data preservation, re-use and open access policy" (https://cms-docdb.cern.ch/cgibin/PublicDocDB/RetrieveFile?docid=6032\&filename=CMSDataPolicyV1.2.pdf\&version=2)].

Compliance with ethical standards

Conflict of interest The authors declare that they have no conflict of interest.

References

1. P.D.B. Collins, *An Introduction to Regge Theory and High-Energy Physics. Cambridge Monographs on Mathematical Physics* (Cambridge University Press, Cambridge, 2009). ISBN:9780521110358
2. H1 Collaboration, Measurement and QCD analysis of the diffractive deep-inelastic scattering cross section at HERA. Eur. Phys. J. C **48**, 715 (2006). https://doi.org/10.1140/epjc/s10052-006-0035-3. arXiv:hep-ex/0606004
3. H1 Collaboration, Diffractive deep-inelastic scattering with a leading proton at HERA. Eur. Phys. J. C **48**, 749 (2006). https://doi.org/10.1140/epjc/s10052-006-0046-0. arXiv:hep-ex/0606003
4. ZEUS Collaboration, Deep inelastic scattering with leading protons or large rapidity gaps at HERA. Nucl. Phys. B **816**, 1 (2009). https://doi.org/10.1016/j.nuclphysb.2009.03.003. arXiv:0812.2003
5. ZEUS Collaboration, A QCD analysis of ZEUS diffractive data. Nucl. Phys. B **831**, 1 (2010). https://doi.org/10.1016/j.nuclphysb.2010.01.014. arXiv:0911.4119
6. UA8 Collaboration, Evidence for a super-hard pomeron structure. Phys. Lett. B **297**, 417 (1992). https://doi.org/10.1016/0370-2693(92)91281-D
7. CDF Collaboration, Measurement of diffractive dijet production at the Fermilab Tevatron. Phys. Rev. Lett. **79**, 2636 (1997). https://doi.org/10.1103/PhysRevLett.79.2636
8. D0 Collaboration, Hard single diffraction in $\bar{p}p$ collisions at $\sqrt{s} =$ 630 and 1800 GeV. Phys. Lett. B **531**, 52 (2002). https://doi.org/10.1016/S0370-2693(02)01364-3. arXiv:hep-ex/9912061

9. CDF Collaboration, Diffractive dijets with a leading antiproton in $\bar{p}p$ collisions at $\sqrt{s} = 1800$ GeV. Phys. Rev. Lett. **84**, 5043 (2000). https://doi.org/10.1103/PhysRevLett.84.5043

10. CDF Collaboration, Diffractive dijet production in $\bar{p}p$ collisions at $\sqrt{s} = 1.96$ TeV. Phys. Rev. D **86**, 032009 (2012). https://doi.org/10.1103/PhysRevD.86.032009. arXiv:1206.3955

11. CDF Collaboration, Diffractive dijet production at $\sqrt{s} = 630$ and $\sqrt{s} = 1800$ GeV at the Fermilab Tevatron. Phys. Rev. Lett. **88**, 151802 (2002). https://doi.org/10.1103/PhysRevLett.88.151802. arXiv:hep-ex/0109025

12. CMS Collaboration, Observation of a diffractive contribution to dijet production in proton–proton collisions at $\sqrt{s} = 7$ TeV. Phys. Rev. D **87**, 012006 (2013). https://doi.org/10.1103/PhysRevD.87.012006. arXiv:1209.1805

13. ATLAS Collaboration, Dijet production in $\sqrt{s} = 7$ TeV pp collisions with large rapidity gaps at the ATLAS experiment. Phys. Lett. B **754**, 214 (2016). https://doi.org/10.1016/j.physletb.2016.01.028. arXiv:1511.00502

14. H1 Collaboration, Diffractive dijet photoproduction in ep collisions at HERA. Eur. Phys. J. C **70**, 15 (2010). https://doi.org/10.1140/epjc/s10052-010-1448-6. arXiv:1006.0946

15. L. Trentadue, G. Veneziano, Fracture functions. An improved description of inclusive hard processes in QCD. Phys. Lett. B **323**, 201 (1994). https://doi.org/10.1016/0370-2693(94)90292-5

16. J.C. Collins, Proof of factorization for diffractive hard scattering. Phys. Rev. D **57**, 3051 (1998). https://doi.org/10.1103/PhysRevD.57.3051. arXiv:hep-ph/9709499 [Erratum: https://doi.org/10.1103/PhysRevD.61.019902]

17. M. Grazzini, L. Trentadue, G. Veneziano, Fracture functions from cut vertices. Nucl. Phys. B **519**, 394 (1998). https://doi.org/10.1016/S0550-3213(97)00840-7. arXiv:hep-ph/9709452

18. J.D. Bjorken, Rapidity gaps and jets as a new-physics signature in very high-energy hadron–hadron collisions. Phys. Rev. D **47**, 101 (1993). https://doi.org/10.1103/PhysRevD.47.101

19. CMS Collaboration, Particle-flow reconstruction and global event description with the CMS detector. JINST **12**, P10003 (2017). https://doi.org/10.1088/1748-0221/12/10/P10003. arXiv:1706.04965

20. M. Cacciari, G.P. Salam, G. Soyez, The anti-k_t jet clustering algorithm. JHEP **04**, 063 (2008). https://doi.org/10.1088/1126-6708/2008/04/063. arXiv:0802.1189

21. M. Cacciari, G.P. Salam, G. Soyez, FastJet user manual. Eur. Phys. J. C **72**, 1896 (2012). https://doi.org/10.1140/epjc/s10052-012-1896-2. arXiv:1111.6097

22. CMS Collaboration, Jet energy scale and resolution in the CMS experiment in pp collisions at 8 TeV. JINST **12**, P02014 (2017). https://doi.org/10.1088/1748-0221/12/02/P02014. arXiv:1607.03663

23. CMS Collaboration, Identification and filtering of uncharacteristic noise in the CMS hadron calorimeter. JINST **5**, T03014 (2010). https://doi.org/10.1088/1748-0221/5/03/T03014. arXiv:0911.4881

24. CMS Collaboration, The CMS experiment at the CERN LHC. JINST **3**, S08004 (2008). https://doi.org/10.1088/1748-0221/3/08/S08004

25. TOTEM Collaboration, The TOTEM experiment at the CERN Large Hadron Collider. JINST **3**, S08007 (2008). https://doi.org/10.1088/1748-0221/3/08/S08007

26. TOTEM Collaboration, Performance of the TOTEM detectors at the LHC. Int. J. Mod. Phys. A **28**, 1330046 (2013). https://doi.org/10.1142/S0217751X13300469. arXiv:1310.2908

27. TOTEM Collaboration, LHC optics measurement with proton tracks detected by the roman pots of the TOTEM experiment. New J. Phys. **16**, 103041 (2014). https://doi.org/10.1088/1367-2630/16/10/103041. arXiv:1406.0546

28. H. Niewiadomski, Reconstruction of protons in the TOTEM roman pot detectors at the LHC. Ph.D. thesis, University of Manchester (2008). http://cds.cern.ch/record/1131825

29. TOTEM Collaboration, Evidence for non-exponential elastic proton–proton differential cross-section at low $|t|$ and $\sqrt{s} = 8$ TeV by TOTEM. Nucl. Phys. B **899**, 527 (2015). https://doi.org/10.1016/j.nuclphysb.2015.08.010. arXiv:1503.08111

30. T. Sjöstrand, S. Mrenna, P. Skands, PYTHIA 6.4 physics and manual. JHEP **05**, 026 (2006). https://doi.org/10.1088/1126-6708/2006/05/026. arXiv:hep-ph/0603175

31. T. Sjöstrand, S. Mrenna, P. Skands, A brief introduction to PYTHIA 8.1. Comput. Phys. Commun. **178**, 852 (2008). https://doi.org/10.1016/j.cpc.2008.01.036. arXiv:0710.3820

32. G. Corcella et al., HERWIG 6: an event generator for hadron emission reactions with interfering gluons (including supersymmetric processes). JHEP **01**, 010 (2001). https://doi.org/10.1088/1126-6708/2001/01/010. arXiv:hep-ph/0011363

33. R. Field, Early LHC underlying event data—findings and surprises. In *Hadron Collider Physics. Proceedings, 22nd Conference, HCP 2010, Toronto, Canada, August 23*, vol. 27 (2010). arXiv:1010.3558

34. R. Corke, T. Sjöstrand, Interleaved parton showers and tuning prospects. JHEP **03**, 032 (2011). https://doi.org/10.1007/JHEP03(2011)032. arXiv:1011.1759

35. CMS Collaboration, Event generator tunes obtained from underlying event and multiparton scattering measurements. Eur. Phys. J. C **76**, 155 (2016). https://doi.org/10.1140/epjc/s10052-016-3988-x. arXiv:1512.00815

36. B. Cox, J. Forshaw, Pomwig: Herwig for diffractive interactions. Comput. Phys. Commun. **144**, 104 (2002). https://doi.org/10.1016/S0010-4655(01)00467-2. arXiv:hep-ph/0010303

37. S. Navin, Diffraction in PYTHIA (2010). arXiv:1005.3894

38. C.O. Rasmussen, T. Sjöstrand, Hard diffraction with dynamic gap survival. JHEP **02**, 142 (2016). https://doi.org/10.1007/JHEP02(2016)142. arXiv:1512.05525

39. CMS and TOTEM Collaboration, Measurement of pseudorapidity distributions of charged particles in proton–proton collisions at $\sqrt{s} = 8$ TeV by the CMS and TOTEM experiments. Eur. Phys. J. C **74**, 3053 (2014). https://doi.org/10.1140/epjc/s10052-014-3053-6. arXiv:1405.0722

40. CMS Collaboration, Measurement of charged particle spectra in minimum-bias events from proton–proton collisions at $\sqrt{s} = 13$ TeV. Eur. Phys. J. C **78**, 697 (2018). https://doi.org/10.1140/epjc/s10052-018-6144-y. arXiv:1806.11245

41. GEANT4 Collaboration, GEANT4 – a simulation toolkit. Nucl. Instrum. Methods A **506**, 250 (2003). https://doi.org/10.1016/S0168-9002(03)01368-8

42. CMS Collaboration, The CMS trigger system. JINST **12**, P01020 (2017). https://doi.org/10.1088/1748-0221/12/01/P01020. arXiv:1609.02366

43. G. D'Agostini, A multidimensional unfolding method based on Bayes' theorem. Nucl. Instrum. Methods A **362**, 487 (1995). https://doi.org/10.1016/0168-9002(95)00274-X

44. CMS Collaboration, Measurement of energy flow at large pseudorapidities in pp collisions at $\sqrt{s} = 0.9$ and 7 TeV. JHEP **11**, 148 (2011). https://doi.org/10.1007/JHEP11(2011)148. arXiv:1110.0211 (**Erratum:** https://doi.org/10.1007/JHEP02(2012)055)

CMS and TOTEM Collaborations

Yerevan Physics Institute, Yerevan, Armenia
A. M. Sirunyan, A. Tumasyan

Institut für Hochenergiephysik, Vienna, Austria
W. Adam, F. Ambrogi, E. Asilar, T. Bergauer, J. Brandstetter, M. Dragicevic, J. Erö, A. Escalante Del Valle,
M. Flechl, R. Frühwirth[1], V. M. Ghete, J. Hrubec, M. Jeitler[1], N. Krammer, I. Krätschmer, D. Liko, T. Madlener,
I. Mikulec, N. Rad, H. Rohringer, J. Schieck[1], R. Schöfbeck, M. Spanring, D. Spitzbart, W. Waltenberger,
J. Wittmann, C.-E. Wulz[1], M. Zarucki
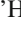
Institute for Nuclear Problems, Minsk, Belarus
V. Chekhovsky, V. Mossolov, J. Suarez Gonzalez

Universiteit Antwerpen, Antwerp, Belgium
E. A. De Wolf, D. Di Croce, X. Janssen, J. Lauwers, A. Lelek, M. Pieters, H. Van Haevermaet, P. Van Mechelen,
N. Van Remortel
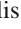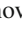
Vrije Universiteit Brussel, Brussels, Belgium
S. Abu Zeid, F. Blekman, J. D'Hondt, J. De Clercq, K. Deroover, G. Flouris, D. Lontkovskyi, S. Lowette,
I. Marchesini, S. Moortgat, L. Moreels, Q. Python, K. Skovpen, S. Tavernier, W. Van Doninck, P. Van Mulders,
I. Van Parijs

Université Libre de Bruxelles, Brussels, Belgium
D. Beghin, B. Bilin, H. Brun, B. Clerbaux, G. De Lentdecker, H. Delannoy, B. Dorney, G. Fasanella, L. Favart,
A. Grebenyuk, A. K. Kalsi, T. Lenzi, J. Luetic, N. Postiau, E. Starling, L. Thomas, C. Vander Velde, P. Vanlaer,
D. Vannerom, Q. Wang

Ghent University, Ghent, Belgium
T. Cornelis, D. Dobur, A. Fagot, M. Gul, I. Khvastunov[2], D. Poyraz, C. Roskas, D. Trocino, M. Tytgat,
W. Verbeke, B. Vermassen, M. Vit, N. Zaganidis

Université Catholique de Louvain, Louvain-la-Neuve, Belgium
H. Bakhshiansohi, O. Bondu, G. Bruno, C. Caputo, P. David, C. Delaere, M. Delcourt, A. Giammanco,
G. Krintiras, V. Lemaitre, A. Magitteri, K. Piotrzkowski, A. Saggio, M. Vidal Marono, P. Vischia, J. Zobec
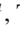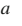
Centro Brasileiro de Pesquisas Fisicas, Rio de Janeiro, Brazil
F. L. Alves, G. A. Alves, G. Correia Silva, C. Hensel, A. Moraes, M. E. Pol, P. Rebello Teles

Universidade do Estado do Rio de Janeiro, Rio de Janeiro, Brazil
E. Belchior Batista Das Chagas, W. Carvalho, J. Chinellato[3], E. Coelho, E. M. Da Costa, G. G. Da Silveira[4],
D. De Jesus Damiao, C. De Oliveira Martins, S. Fonseca De Souza, L. M. Huertas Guativa, H. Malbouisson,
D. Matos Figueiredo, M. Melo De Almeida, C. Mora Herrera, L. Mundim, H. Nogima, W. L. Prado Da Silva,
L. J. Sanchez Rosas, A. Santoro, A. Sznajder, M. Thiel, E. J. Tonelli Manganote[3], F. Torres Da Silva De Araujo,
A. Vilela Pereira

Universidade Estadual Paulista[a], Universidade Federal do ABC[b], São Paulo, Brazil
S. Ahuja[a], C. A. Bernardes[a], L. Calligaris[a], T. R. Fernandez Perez Tomei[a], E. M. Gregores[b],
P. G. Mercadante[b], S. F. Novaes[a], SandraS. Padula[a]

Institute for Nuclear Research and Nuclear Energy, Bulgarian Academy of Sciences, Sofia, Bulgaria
A. Aleksandrov, R. Hadjiiska, P. Iaydjiev, A. Marinov, M. Misheva, M. Rodozov, M. Shopova, G. Sultanov

University of Sofia, Sofia, Bulgaria
A. Dimitrov, L. Litov, B. Pavlov, P. Petkov

Beihang University, Beijing, China
W. Fang[5], X. Gao[5], L. Yuan[5]

Department of Physics, Tsinghua University, Beijing, China
Y. Wang

Institute of High Energy Physics, Beijing, China
M. Ahmad, J. G. Bian, G. M. Chen, H. S. Chen, M. Chen, Y. Chen, C. H. Jiang, D. Leggat, H. Liao, Z. Liu, S. M. Shaheen[6], A. Spiezia, J. Tao, E. Yazgan, H. Zhang, S. Zhang[6], J. Zhao

State Key Laboratory of Nuclear Physics and Technology, Peking University, Beijing, China
Y. Ban, G. Chen, A. Levin, J. Li, L. Li, Q. Li, Y. Mao, S. J. Qian, D. Wang

Universidad de Los Andes, Bogota, Colombia
C. Avila, A. Cabrera, C. A. Carrillo Montoya, L. F. Chaparro Sierra, C. Florez, C. F. González Hernández, M. A. Segura Delgado

University of Split, Faculty of Electrical Engineering, Mechanical Engineering and Naval Architecture, Split, Croatia
B. Courbon, N. Godinovic, D. Lelas, I. Puljak, T. Sculac

University of Split, Faculty of Science, Split, Croatia
Z. Antunovic, M. Kovac

Institute Rudjer Boskovic, Zagreb, Croatia
V. Brigljevic, D. Ferencek, K. Kadija, B. Mesic, M. Roguljic, A. Starodumov[7], T. Susa

University of Cyprus, Nicosia, Cyprus
M. W. Ather, A. Attikis, M. Kolosova, G. Mavromanolakis, J. Mousa, C. Nicolaou, F. Ptochos, P. A. Razis, H. Rykaczewski

Charles University, Prague, Czech Republic
M. Finger[8], M. Finger Jr.[8]

Escuela Politecnica Nacional, Quito, Ecuador
E. Ayala

Universidad San Francisco de Quito, Quito, Ecuador
E. Carrera Jarrin

Academy of Scientific Research and Technology of the Arab Republic of Egypt, Egyptian Network of High Energy Physics, Cairo, Egypt
A. Ellithi Kamel[9], M. A. Mahmoud[10,11], E. Salama[11,12]

National Institute of Chemical Physics and Biophysics, Tallinn, Estonia
S. Bhowmik, A. Carvalho Antunes De Oliveira, R. K. Dewanjee, K. Ehataht, M. Kadastik, M. Raidal, C. Veelken

Department of Physics, University of Helsinki, Helsinki, Finland
P. Eerola, H. Kirschenmann, J. Pekkanen, M. Voutilainen

Helsinki Institute of Physics, Helsinki, Finland
J. Havukainen, J. K. Heikkilä, T. Järvinen, V. Karimäki, R. Kinnunen, T. Lampén, K. Lassila-Perini, S. Laurila, S. Lehti, T. Lindén, P. Luukka, T. Mäenpää, H. Siikonen, E. Tuominen, J. Tuominiemi

Lappeenranta University of Technology, Lappeenranta, Finland
T. Tuuva

IRFU, CEA, Université Paris-Saclay, Gif-sur-Yvette, France
M. Besancon, F. Couderc, M. Dejardin, D. Denegri, J. L. Faure, F. Ferri, S. Ganjour, A. Givernaud, P. Gras, G. Hamel de Monchenault, P. Jarry, C. Leloup, E. Locci, J. Malcles, G. Negro, J. Rander, A. Rosowsky, M.Ö. Sahin, M. Titov

Laboratoire Leprince-Ringuet, CNRS/IN2P3, Ecole Polytechnique, Institut Polytechnique de Paris, Paris, France
A. Abdulsalam[13], C. Amendola, I. Antropov, F. Beaudette, P. Busson, C. Charlot, R. Granier de Cassagnac, I. Kucher, A. Lobanov, J. Martin Blanco, C. Martin Perez, M. Nguyen, C. Ochando, G. Ortona, P. Paganini, J. Rembser, R. Salerno, J. B. Sauvan, Y. Sirois, A. G. Stahl Leiton, A. Zabi, A. Zghiche

Université de Strasbourg, CNRS, IPHC UMR 7178, Strasbourg, France

J.-L. Agram [14], J. Andrea, D. Bloch, G. Bourgatte, J.-M. Brom, E. C. Chabert, V. Cherepanov, C. Collard, E. Conte [14], J.-C. Fontaine [14], D. Gelé, U. Goerlach, M. Jansová, A.-C. Le Bihan, N. Tonon, P. Van Hove

Centre de Calcul de l'Institut National de Physique Nucleaire et de Physique des Particules, CNRS/IN2P3, Villeurbanne, France

S. Gadrat

Université de Lyon, Université Claude Bernard Lyon 1, CNRS-IN2P3, Institut de Physique Nucléaire de Lyon, Villeurbanne, France

S. Beauceron, C. Bernet, G. Boudoul, N. Chanon, R. Chierici, D. Contardo, P. Depasse, H. El Mamouni, J. Fay, L. Finco, S. Gascon, M. Gouzevitch, G. Grenier, B. Ille, F. Lagarde, I. B. Laktineh, H. Lattaud, M. Lethuillier, L. Mirabito, S. Perries, A. Popov [15], V. Sordini, G. Touquet, M. Vander Donckt, S. Viret

Georgian Technical University, Tbilisi, Georgia

T. Toriashvili [16]

Tbilisi State University, Tbilisi, Georgia

Z. Tsamalaidze [8]

RWTH Aachen University, I. Physikalisches Institut, Aachen, Germany

C. Autermann, L. Feld, M. K. Kiesel, K. Klein, M. Lipinski, M. Preuten, M. P. Rauch, C. Schomakers, J. Schulz, M. Teroerde, B. Wittmer
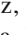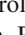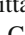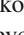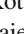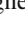
RWTH Aachen University, III. Physikalisches Institut A, Aachen, Germany

A. Albert, M. Erdmann, S. Erdweg, T. Esch, R. Fischer, S. Ghosh, A. Güth, T. Hebbeker, C. Heidemann, K. Hoepfner, H. Keller, L. Mastrolorenzo, M. Merschmeyer, A. Meyer, P. Millet, S. Mukherjee, T. Pook, M. Radziej, H. Reithler, M. Rieger, A. Schmidt, D. Teyssier, S. Thüer
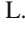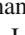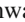
RWTH Aachen University, III. Physikalisches Institut B, Aachen, Germany

G. Flügge, O. Hlushchenko, T. Kress, T. Müller, A. Nehrkorn, A. Nowack, C. Pistone, O. Pooth, D. Roy, H. Sert, A. Stahl [17]

Deutsches Elektronen-Synchrotron, Hamburg, Germany

M. Aldaya Martin, T. Arndt, C. Asawatangtrakuldee, I. Babounikau, K. Beernaert, O. Behnke, U. Behrens, A. Bermúdez Martínez, D. Bertsche, A. A. Bin Anuar, K. Borras [18], V. Botta, A. Campbell, P. Connor, C. Contreras-Campana, V. Danilov, A. De Wit, M. M. Defranchis, C. Diez Pardos, D. Domínguez Damiani, G. Eckerlin, T. Eichhorn, A. Elwood, E. Eren, E. Gallo [19], A. Geiser, J. M. Grados Luyando, A. Grohsjean, M. Guthoff, M. Haranko, A. Harb, H. Jung, M. Kasemann, J. Keaveney, C. Kleinwort, J. Knolle, D. Krücker, W. Lange, T. Lenz, J. Leonard, K. Lipka, W. Lohmann [20], R. Mankel, I.-A. Melzer-Pellmann, A. B. Meyer, M. Meyer, M. Missiroli, G. Mittag, J. Mnich, V. Myronenko, S. K. Pflitsch, D. Pitzl, A. Raspereza, A. Saibel, M. Savitskyi, P. Saxena, P. Schütze, C. Schwanenberger, R. Shevchenko, A. Singh, H. Tholen, O. Turkot, A. Vagnerini, M. Van De Klundert, G. P. Van Onsem, R. Walsh, Y. Wen, K. Wichmann, C. Wissing, O. Zenaiev

University of Hamburg, Hamburg, Germany

R. Aggleton, S. Bein, L. Benato, A. Benecke, T. Dreyer, A. Ebrahimi, E. Garutti, D. Gonzalez, P. Gunnellini, J. Haller, A. Hinzmann, A. Karavdina, G. Kasieczka, R. Klanner, R. Kogler, N. Kovalchuk, S. Kurz, V. Kutzner, J. Lange, D. Marconi, J. Multhaup, M. Niedziela, C. E. N. Niemeyer, D. Nowatschin, A. Perieanu, A. Reimers, O. Rieger, C. Scharf, P. Schleper, S. Schumann, J. Schwandt, J. Sonneveld, H. Stadie, G. Steinbrück, F. M. Stober, M. Stöver, B. Vormwald, I. Zoi

Karlsruher Institut fuer Technologie, Karlsruhe, Germany

M. Akbiyik, C. Barth, M. Baselga, S. Baur, E. Butz, R. Caspart, T. Chwalek, F. Colombo, W. De Boer, A. Dierlamm, K. El Morabit, N. Faltermann, B. Freund, M. Giffels, M. A. Harrendorf, F. Hartmann [17], S. M. Heindl, U. Husemann, I. Katkov [15], S. Kudella, S. Mitra, M. U. Mozer, Th. Müller, M. Musich, M. Plagge, G. Quast, K. Rabbertz, M. Schröder, I. Shvetsov, H. J. Simonis, R. Ulrich, S. Wayand, M. Weber, T. Weiler, C. Wöhrmann, R. Wolf

Institute of Nuclear and Particle Physics (INPP), NCSR Demokritos, Aghia Paraskevi, Greece
G. Anagnostou, G. Daskalakis, T. Geralis, A. Kyriakis, D. Loukas, G. Paspalaki

National and Kapodistrian University of Athens, Athens, Greece
A. Agapitos, G. Karathanasis, P. Kontaxakis, A. Panagiotou, I. Papavergou, N. Saoulidou, K. Vellidis

National Technical University of Athens, Athens, Greece
K. Kousouris , I. Papakrivopoulos, G. Tsipolitis

University of Ioánnina, Ioánnina, Greece
I. Evangelou, C. Foudas, P. Gianneios, P. Katsoulis, P. Kokkas, S. Mallios, N. Manthos, I. Papadopoulos, E. Paradas, J. Strologas , F. A. Triantis, D. Tsitsonis

MTA-ELTE Lendület CMS Particle and Nuclear Physics Group, Eötvös Loránd University, Budapest, Hungary
M. Bartók[21], M. Csanad , N. Filipovic, P. Major, M. I. Nagy, G. Pasztor , O. Surányi, G. I. Veres

Wigner Research Centre for Physics, Budapest, Hungary
G. Bencze, C. Hajdu , D. Horvath[22], Á. Hunyadi, F. Sikler , T.Á. Vámi , V. Veszpremi, G. Vesztergombi[†]

Institute of Nuclear Research ATOMKI, Debrecen, Hungary
N. Beni, S. Czellar, J. Karancsi[21], A. Makovec , J. Molnar, Z. Szillasi

Institute of Physics, University of Debrecen, Debrecen, Hungary
P. Raics, Z. L. Trocsanyi , B. Ujvari

Indian Institute of Science (IISc), Bangalore, India
S. Choudhury, J. R. Komaragiri , P. C. Tiwari

National Institute of Science Education and Research, HBNI, Bhubaneswar, India
S. Bahinipati[24], C. Kar, P. Mal, K. Mandal, A. Nayak[25], S. Roy Chowdhury, D. K. Sahoo[24], S. K. Swain

Panjab University, Chandigarh, India
S. Bansal , S. B. Beri, V. Bhatnagar, S. Chauhan, R. Chawla, N. Dhingra, R. Gupta, A. Kaur, M. Kaur, S. Kaur, P. Kumari, M. Lohan, M. Meena, A. Mehta , K. Sandeep, S. Sharma, J. B. Singh, A. K. Virdi, G. Walia

University of Delhi, Delhi, India
A. Bhardwaj, B. C. Choudhary , R. B. Garg, M. Gola, S. Keshri , Ashok Kumar, S. Malhotra, M. Naimuddin , P. Priyanka, K. Ranjan, Aashaq Shah, R. Sharma

Saha Institute of Nuclear Physics, HBNI, Kolkata, India
R. Bhardwaj[26], M. Bharti[26], R. Bhattacharya, S. Bhattacharya, U. Bhawandeep[26], D. Bhowmik, S. Dey, S. Dutt[26], S. Dutta, S. Ghosh, M. Maity[27], K. Mondal, S. Nandan, A. Purohit, P. K. Rout, A. Roy, G. Saha, S. Sarkar, T. Sarkar [27], M. Sharan, B. Singh[26], S. Thakur[26]

Indian Institute of Technology Madras, Madras, India
P. K. Behera , A. Muhammad

Bhabha Atomic Research Centre, Mumbai, India
R. Chudasama, D. Dutta, V. Jha, V. Kumar, D. K. Mishra, P. K. Netrakanti, L. M. Pant, P. Shukla , P. Suggisetti
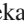
Tata Institute of Fundamental Research-A, Mumbai, India
T. Aziz, M. A. Bhat, S. Dugad, G. B. Mohanty , N. Sur , Ravindra Kumar Verma

Tata Institute of Fundamental Research-B, Mumbai, India
S. Banerjee, S. Bhattacharya, S. Chatterjee, P. Das, M. Guchait, Sa. Jain , S. Karmakar, S. Kumar, G. Majumder, K. Mazumdar, N. Sahoo

Indian Institute of Science Education and Research (IISER), Pune, India
S. Chauhan , S. Dube , V. Hegde, A. Kapoor , K. Kothekar , S. Pandey, A. Rane, A. Rastogi, S. Sharma
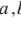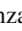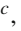
Institute for Research in Fundamental Sciences (IPM), Tehran, Iran

S. Chenarani[28], E. Eskandari Tadavani, S. M. Etesami[28], M. Khakzad, M. Mohammadi Najafabadi, M. Naseri, F. Rezaei Hosseinabadi, B. Safarzadeh[29], M. Zeinali
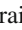
University College Dublin, Dublin, Ireland

M. Felcini, M. Grunewald

INFN Sezione di Bari[a]**, Università di Bari**[b]**, Politecnico di Bari**[c]**, Bari, Italy**

M. Abbrescia[a,b], C. Calabria[a,b], A. Colaleo[a], D. Creanza[a,c], L. Cristella[a,b], N. De Filippis[a,c], M. De Palma[a,b], A. Di Florio[a,b], F. Errico[a,b], L. Fiore[a], A. Gelmi[a,b], G. Iaselli[a,c], M. Ince[a,b], S. Lezki[a,b], G. Maggi[a,c], M. Maggi[a], G. Miniello[a,b], S. My[a,b], S. Nuzzo[a,b], A. Pompili[a,b], G. Pugliese[a,c], R. Radogna[a], A. Ranieri[a], G. Selvaggi[a,b], A. Sharma[a], L. Silvestris[a], R. Venditti[a], P. Verwilligen[a]

INFN Sezione di Bologna[a]**, Università di Bologna**[b]**, Bologna, Italy**

G. Abbiendi[a], C. Battilana[a,b], D. Bonacorsi[a,b], L. Borgonovi[a,b], S. Braibant-Giacomelli[a,b], R. Campanini[a,b], P. Capiluppi[a,b], A. Castro[a,b], F. R. Cavallo[a], S. S. Chhibra[a,b], G. Codispoti[a,b], M. Cuffiani[a,b], G. M. Dallavalle[a], F. Fabbri[a], A. Fanfani[a,b], E. Fontanesi, P. Giacomelli[a], C. Grandi[a], L. Guiducci[a,b], F. Iemmi[a,b], S. Lo Meo[a,30], S. Marcellini[a], G. Masetti[a], A. Montanari[a], F. L. Navarria[a,b], A. Perrotta[a], F. Primavera[a,b], A. M. Rossi[a,b], T. Rovelli[a,b], G. P. Siroli[a,b], N. Tosi[a]

INFN Sezione di Catania[a]**, Università di Catania**[b]**, Catania, Italy**

S. Albergo[a,b], A. Di Mattia[a], R. Potenza[a,b], A. Tricomi[a,b], C. Tuve[a,b]

INFN Sezione di Firenze[a]**, Università di Firenze**[b]**, Florence, Italy**

G. Barbagli[a], K. Chatterjee[a,b], V. Ciulli[a,b], C. Civinini[a], R. D'Alessandro[a,b], E. Focardi[a,b], G. Latino, P. Lenzi[a,b], M. Meschini[a], S. Paoletti[a], L. Russo[a,31], G. Sguazzoni[a], D. Strom[a], L. Viliani[a]
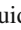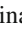
INFN Laboratori Nazionali di Frascati, Frascati, Italy

L. Benussi, S. Bianco, F. Fabbri, D. Piccolo

INFN Sezione di Genova[a]**, Università di Genova**[b]**, Genoa, Italy**

F. Ferro[a], R. Mulargia[a,b], E. Robutti[a], S. Tosi[a,b]
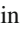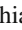
INFN Sezione di Milano-Bicocca[a]**, Università di Milano-Bicocca**[b]**, Milan, Italy**

A. Benaglia[a], A. Beschi[b], F. Brivio[a,b], V. Ciriolo[a,b,17], S. Di Guida[a,b,17], M. E. Dinardo[a,b], S. Fiorendi[a,b], S. Gennai[a], A. Ghezzi[a,b], P. Govoni[a,b], M. Malberti[a,b], S. Malvezzi[a], D. Menasce[a], F. Monti, L. Moroni[a], M. Paganoni[a,b], D. Pedrini[a], S. Ragazzi[a,b], T. Tabarelli de Fatis[a,b], D. Zuolo[a,b]

INFN Sezione di Napoli[a]**, Università di Napoli 'Federico II'**[b]**, Naples, Italy, Università della Basilicata**[c]**, Potenza, Italy, Università G. Marconi**[d]**, Rome, Italy**

S. Buontempo[a], N. Cavallo[a,c], A. De Iorio[a,b], A. Di Crescenzo[a,b], F. Fabozzi[a,c], F. Fienga[a], G. Galati[a], A. O. M. Iorio[a,b], L. Lista[a], S. Meola[a,d,17], P. Paolucci[a,17], C. Sciacca[a,b], E. Voevodina[a,b]
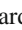
INFN Sezione di Padova[a]**, Università di Padova**[b]**, Padoa, Italy, Università di Trento**[c]**, Trento, Italy**

P. Azzi[a], N. Bacchetta[a], D. Bisello[a,b], A. Boletti[a,b], A. Bragagnolo, R. Carlin[a,b], P. Checchia[a], M. Dall'Osso[a,b], P. De Castro Manzano[a], T. Dorigo[a], U. Dosselli[a], F. Gasparini[a,b], U. Gasparini[a,b], A. Gozzelino[a], S. Y. Hoh, S. Lacaprara[a], P. Lujan, M. Margoni[a,b], A. T. Meneguzzo[a,b], J. Pazzini[a,b], M. Presilla[b], P. Ronchese[a,b], R. Rossin[a,b], F. Simonetto[a,b], A. Tiko, E. Torassa[a], M. Tosi[a,b], M. Zanetti[a,b], P. Zotto[a,b], G. Zumerle[a,b]
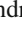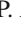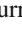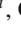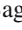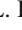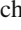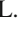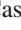
INFN Sezione di Pavia[a]**, Università di Pavia**[b]**, Pavia, Italy**

A. Braghieri[a], A. Magnani[a], P. Montagna[a,b], S. P. Ratti[a,b], V. Re[a], M. Ressegotti[a,b], C. Riccardi[a,b], P. Salvini[a], I. Vai[a,b], P. Vitulo[a,b]
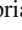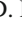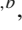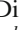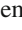
INFN Sezione di Perugia[a]**, Università di Perugia**[b]**, Perugia, Italy**

M. Biasini[a,b], G. M. Bilei[a], C. Cecchi[a,b], D. Ciangottini[a,b], L. Fanò[a,b], P. Lariccia[a,b], R. Leonardi[a,b], E. Manoni[a], G. Mantovani[a,b], V. Mariani[a,b], M. Menichelli[a], A. Rossi[a,b], A. Santocchia[a,b], D. Spiga[a]
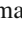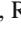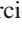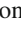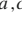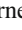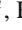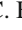
INFN Sezione di Pisa^a, Università di Pisa^b, Scuola Normale Superiore di Pisa^c, Pisa, Italy

K. Androsov ^{a}, P. Azzurri ^{a}, G. Bagliesi ^{a}, L. Bianchini ^{a}, T. Boccali ^{a}, L. Borrello , R. Castaldi ^{a}, M. A. Ciocci ^{a,b}, R. Dell'Orso ^{a}, G. Fedi ^{a}, F. Fiori^{a,c}, L. Giannini^{a,c}, A. Giassi ^{a}, M. T. Grippo ^{a}, F. Ligabue ^{a,c}, E. Manca ^{a,c}, G. Mandorli^{a,c}, A. Messineo ^{a,b}, F. Palla ^{a}, A. Rizzi ^{a,b}, G. Rolandi ^{32}, P. Spagnolo ^{a}, R. Tenchini ^{a}, G. Tonelli ^{a,b}, A. Venturi ^{a}, P. G. Verdini ^{a}
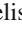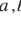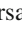
INFN Sezione di Roma^a, Sapienza Università di Roma^b, Rome, Italy

L. Barone^{a,b}, F. Cavallari ^{a}, M. Cipriani ^{a,b}, D. Del Re ^{a,b}, E. Di Marco^{a,b}, M. Diemoz ^{a}, S. Gelli ^{a,b}, E. Longo ^{a,b}, B. Marzocchi ^{a,b}, P. Meridiani ^{a}, G. Organtini ^{a,b}, F. Pandolfi^a, R. Paramatti ^{a,b}, F. Preiato ^{a,b}, S. Rahatlou ^{a,b}, C. Rovelli ^{a}, F. Santanastasio ^{a,b}
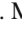
INFN Sezione di Torino^a, Università di Torino^b, Turin, Italy, Università del Piemonte Orientale^c, Novara, Italy

N. Amapane ^{a,b}, R. Arcidiacono ^{a,c}, S. Argiro ^{a,b}, M. Arneodo ^{a,c}, N. Bartosik^a, R. Bellan ^{a,b}, C. Biino ^{a}, A. Cappati^{a,b}, N. Cartiglia ^{a}, F. Cenna^{a,b}, S. Cometti ^{a}, M. Costa ^{a,b}, R. Covarelli ^{a,b}, N. Demaria ^{a}, B. Kiani^{a,b}, C. Mariotti ^{a}, S. Maselli ^{a}, E. Migliore ^{a,b}, V. Monaco ^{a,b}, E. Monteil ^{a,b}, M. Monteno ^{a}, M. M. Obertino ^{a,b}, L. Pacher ^{a,b}, N. Pastrone ^{a}, M. Pelliccioni ^{a}, G. L. Pinna Angioni^{a,b}, A. Romero^{a,b}, M. Ruspa ^{a,c}, R. Sacchi ^{a,b}, R. Salvatico^{a,b}, K. Shchelina^{a,b}, V. Sola ^{a}, A. Solano^{a,b}, D. Soldi ^{a,b}, A. Staiano ^{a}

INFN Sezione di Trieste^a, Università di Trieste^b, Trieste, Italy

S. Belforte ^{a}, V. Candelise ^{a,b}, M. Casarsa ^{a}, F. Cossutti ^{a}, A. Da Rold ^{a,b}, G. Della Ricca ^{a,b}, F. Vazzoler ^{a,b}, A. Zanetti ^{a}

Kyungpook National University, Daegu, Korea

D. H. Kim, G. N. Kim, M. S. Kim, J. Lee, S. Lee, S. W. Lee , C. S. Moon , Y. D. Oh, S. I. Pak, S. Sekmen , D. C. Son , Y. C. Yang

Chonnam National University, Institute for Universe and Elementary Particles, Kwangju, Korea

H. Kim, D. H. Moon , G. Oh

Hanyang University, Seoul, Korea

B. Francois, J. Goh ^{33}, T. J. Kim

Korea University, Seoul, Korea

S. Cho, S. Choi, Y. Go, D. Gyun, S. Ha, B. Hong , Y. Jo, K. Lee, K. S. Lee, S. Lee, J. Lim, S. K. Park, Y. Roh

Sejong University, Seoul, Korea

H. S. Kim

Seoul National University, Seoul, Korea

J. Almond, J. Kim, J. S. Kim, H. Lee , K. Lee, K. Nam, S. B. Oh, B. C. Radburn-Smith, S.h. Seo , U. K. Yang, H. D. Yoo, G. B. Yu

University of Seoul, Seoul, Korea

D. Jeon, H. Kim, J. H. Kim, J. S. H. Lee , I. C. Park

Sungkyunkwan University, Suwon, Korea

Y. Choi, C. Hwang, J. Lee, I. Yu

Riga Technical University, Riga, Latvia

V. Veckalns ^{34}

Vilnius University, Vilnius, Lithuania

V. Dudenas, A. Juodagalvis , J. Vaitkus

National Centre for Particle Physics, Universiti Malaya, Kuala Lumpur, Malaysia

Z. A. Ibrahim, M. A. B. Md Ali^{35}, F. Mohamad Idris^{36}, W. A. T. Wan Abdullah, M. N. Yusli, Z. Zolkapli

Universidad de Sonora (UNISON), Hermosillo, Mexico

J. F. Benitez , A. Castaneda Hernandez , J. A. Murillo Quijada

Centro de Investigacion y de Estudios Avanzados del IPN, Mexico City, Mexico
H. Castilla-Valdez, E. De La Cruz-Burelo, M. C. Duran-Osuna, I. Heredia-De La Cruz[37], R. Lopez-Fernandez,
J. Mejia Guisao, R. I. Rabadan-Trejo, M. Ramirez-Garcia, G. Ramirez-Sanchez, R. Reyes-Almanza, A. Sanchez-Hernandez

Universidad Iberoamericana, Mexico City, Mexico
S. Carrillo Moreno, C. Oropeza Barrera, F. Vazquez Valencia

Benemerita Universidad Autonoma de Puebla, Puebla, Mexico
J. Eysermans, I. Pedraza, H. A. Salazar Ibarguen, C. Uribe Estrada

Universidad Autónoma de San Luis Potosí, San Luis Potosí, Mexico
A. Morelos Pineda

University of Auckland, Auckland, New Zealand
D. Krofcheck

University of Canterbury, Christchurch, New Zealand
S. Bheesette, P. H. Butler

National Centre for Physics, Quaid-I-Azam University, Islamabad, Pakistan
A. Ahmad, M. Ahmad, M. I. Asghar, Q. Hassan, H. R. Hoorani, W. A. Khan, M. A. Shah, M. Shoaib, M. Waqas

National Centre for Nuclear Research, Swierk, Poland
H. Bialkowska, M. Bluj, B. Boimska, T. Frueboes, M. Górski, M. Kazana, M. Szleper, P. Traczyk, P. Zalewski

Institute of Experimental Physics, Faculty of Physics, University of Warsaw, Warsaw, Poland
K. Bunkowski, A. Byszuk[38], K. Doroba, A. Kalinowski, M. Konecki, J. Krolikowski, M. Misiura, M. Olszewski,
A. Pyskir, M. Walczak

Laboratório de Instrumentação e Física Experimental de Partículas, Lisbon, Portugal
M. Araujo, P. Bargassa, C. Beirão Da Cruz E Silva, A. Di Francesco, P. Faccioli, B. Galinhas, M. Gallinaro,
J. Hollar, N. Leonardo, J. Seixas, G. Strong, O. Toldaiev, J. Varela

Joint Institute for Nuclear Research, Dubna, Russia
S. Afanasiev, P. Bunin, M. Gavrilenko, I. Golutvin, I. Gorbunov, A. Kamenev, V. Karjavine, A. Lanev, A. Malakhov,
V. Matveev[39,40], P. Moisenz, V. Palichik, V. Perelygin, S. Shmatov, S. Shulha, N. Skatchkov, V. Smirnov, N. Voytishin,
A. Zarubin

Petersburg Nuclear Physics Institute, Gatchina (St. Petersburg), Russia
V. Golovtsov, Y. Ivanov, V. Kim[41], E. Kuznetsova[42], P. Levchenko, V. Murzin, V. Oreshkin, I. Smirnov, D. Sosnov,
V. Sulimov, L. Uvarov, S. Vavilov, A. Vorobyev

Institute for Nuclear Research, Moscow, Russia
Yu. Andreev, A. Dermenev, S. Gninenko, N. Golubev, A. Karneyeu, M. Kirsanov, N. Krasnikov, A. Pashenkov,
A. Shabanov, D. Tlisov, A. Toropin

Institute for Theoretical and Experimental Physics named by A.I. Alikhanov of NRC 'Kurchatov Institute', Moscow, Russia
V. Epshteyn, V. Gavrilov, N. Lychkovskaya, V. Popov, I. Pozdnyakov, G. Safronov, A. Spiridonov, A. Stepennov,
V. Stolin, M. Toms, E. Vlasov, A. Zhokin

Moscow Institute of Physics and Technology, Moscow, Russia
T. Aushev

P.N. Lebedev Physical Institute, Moscow, Russia
V. Andreev, M. Azarkin, I. Dremin[40], M. Kirakosyan, A. Terkulov

Skobeltsyn Institute of Nuclear Physics, Lomonosov Moscow State University, Moscow, Russia
A. Belyaev, E. Boos, A. Ershov, A. Gribushin, L. Khein, V. Klyukhin, O. Kodolova, I. Lokhtin, O. Lukina,
S. Obraztsov, S. Petrushanko, V. Savrin, A. Snigirev

Novosibirsk State University (NSU), Novosibirsk, Russia
A. Barnyakov[43], V. Blinov[43], T. Dimova[43], L. Kardapoltsev[43], Y. Skovpen [43]

Institute for High Energy Physics of National Research Centre 'Kurchatov Institute', Protvino, Russia
I. Azhgirey , I. Bayshev, S. Bitioukov , V. Kachanov, A. Kalinin, D. Konstantinov, P. Mandrik, V. Petrov, R. Ryutin,
S. Slabospitskii , A. Sobol, S. Troshin , N. Tyurin, A. Uzunian, A. Volkov

National Research Tomsk Polytechnic University, Tomsk, Russia
A. Babaev, S. Baidali, V. Okhotnikov

University of Belgrade, Faculty of Physics and VINCA Institute of Nuclear Sciences, Belgrade, Serbia
P. Adzic[44], P. Cirkovic , D. Devetak, M. Dordevic , P. Milenovic[45], J. Milosevic

Centro de Investigaciones Energéticas Medioambientales y Tecnológicas (CIEMAT), Madrid, Spain
J. Alcaraz Maestre , A. Álvarez Fernández, I. Bachiller, M. Barrio Luna, J. A. Brochero Cifuentes, M. Cerrada,
N. Colino , B. De La Cruz, A. Delgado Peris , C. Fernandez Bedoya , J. P. Fernández Ramos , J. Flix ,
M. C. Fouz, O. Gonzalez Lopez, S. Goy Lopez, J. M. Hernandez , M. I. Josa, D. Moran, A. Pérez-Calero Yzquierdo,
J. Puerta Pelayo, I. Redondo , L. Romero, S. Sánchez Navas, M. S. Soares , A. Triossi

Universidad Autónoma de Madrid, Madrid, Spain
C. Albajar, J. F. de Trocóniz

Instituto Universitario de Ciencias y Tecnologías Espaciales de Asturias (ICTEA), Universidad de Oviedo, Oviedo, Spain
J. Cuevas , C. Erice, J. Fernandez Menendez, S. Folgueras , I. Gonzalez Caballero , J. R. González Fernández,
E. Palencia Cortezon , V. Rodríguez Bouza , S. Sanchez Cruz , J. M. Vizan Garcia

Instituto de Física de Cantabria (IFCA), CSIC-Universidad de Cantabria, Santander, Spain
I. J. Cabrillo, A. Calderon , B. Chazin Quero, J. Duarte Campderros , M. Fernandez , P. J. Fernández Manteca ,
A. García Alonso, J. Garcia-Ferrero, G. Gomez, A. Lopez Virto, J. Marco, C. Martinez Rivero, P. Martinez Ruiz del Arbol,
F. Matorras , J. Piedra Gomez, C. Prieels, T. Rodrigo , A. Ruiz-Jimeno , L. Scodellaro , N. Trevisani , I. Vila,
R. Vilar Cortabitarte

University of Ruhuna, Department of Physics, Matara, Sri Lanka
N. Wickramage

CERN, European Organization for Nuclear Research, Geneva, Switzerland
D. Abbaneo, B. Akgun, E. Auffray, G. Auzinger, P. Baillon, A. H. Ball, D. Barney, J. Bendavid, M. Bianco , A. Bocci,
C. Botta , E. Brondolin, T. Camporesi, M. Cepeda , G. Cerminara, E. Chapon , Y. Chen , G. Cucciati, D. d'Enterria,
A. Dabrowski, N. Daci, V. Daponte, A. David , A. De Roeck, N. Deelen, M. Dobson, M. Dünser, N. Dupont,
A. Elliott-Peisert, F. Fallavollita[46], D. Fasanella , G. Franzoni , J. Fulcher , W. Funk, D. Gigi, A. Gilbert , K. Gill,
F. Glege, M. Gruchala, M. Guilbaud, D. Gulhan, J. Hegeman , C. Heidegger , V. Innocente, G. M. Innocenti,
A. Jafari , P. Janot , O. Karacheban [20], J. Kieseler , A. Kornmayer, M. Krammer [1], C. Lange, P. Lecoq ,
C. Lourenço , L. Malgeri , M. Mannelli, A. Massironi , F. Meijers, J. A. Merlin, S. Mersi , E. Meschi ,
F. Moortgat , M. Mulders , J. Ngadiuba, S. Nourbakhsh, S. Orfanelli, L. Orsini, F. Pantaleo [17], L. Pape, E. Perez,
M. Peruzzi, A. Petrilli, G. Petrucciani , A. Pfeiffer , M. Pierini , F. M. Pitters, D. Rabady , A. Racz, T. Reis ,
M. Rovere, H. Sakulin, C. Schäfer, C. Schwick, M. Selvaggi, A. Sharma, P. Silva , P. Sphicas [47], A. Stakia,
J. Steggemann , D. Treille, A. Tsirou, A. Vartak , M. Verzetti, W. D. Zeuner

Paul Scherrer Institut, Villigen, Switzerland
L. Caminada [48], K. Deiters, W. Erdmann, R. Horisberger, Q. Ingram, H. C. Kaestli, D. Kotlinski, U. Langenegger,
T. Rohe, S. A. Wiederkehr

ETH Zurich, Institute for Particle Physics and Astrophysics (IPA), Zurich, Switzerland
M. Backhaus [iD], L. Bäni [iD], P. Berger, N. Chernyavskaya, G. Dissertori [iD], M. Dittmar, M. Donegà, C. Dorfer,
T. A. Gómez Espinosa, C. Grab [iD], D. Hits, T. Klijnsma, W. Lustermann, R. A. Manzoni [iD], M. Marionneau,
M. T. Meinhard, F. Micheli, P. Musella [iD], F. Nessi-Tedaldi, F. Pauss, G. Perrin, L. Perrozzi, S. Pigazzini [iD],
M. Reichmann, C. Reissel, D. Ruini, D. A. Sanz Becerra, M. Schönenberger, L. Shchutska [iD], V. R. Tavolaro [iD],
K. Theofilatos, M. L. Vesterbacka Olsson, R. Wallny [iD], D. H. Zhu

Universität Zürich, Zurich, Switzerland
T. K. Aarrestad, C. Amsler[49], D. Brzhechko, M. F. Canelli [iD], A. De Cosa, R. Del Burgo, S. Donato [iD], C. Galloni,
T. Hreus, B. Kilminster [iD], S. Leontsinis [iD], I. Neutelings, G. Rauco, P. Robmann, D. Salerno [iD], K. Schweiger [iD], C. Seitz,
Y. Takahashi [iD], S. Wertz [iD], A. Zucchetta [iD]

National Central University, Chung-Li, Taiwan
T. H. Doan, R. Khurana, C. M. Kuo, W. Lin, A. Pozdnyakov [iD], S. S. Yu

National Taiwan University (NTU), Taipei, Taiwan
P. Chang, Y. Chao, K. F. Chen, P. H. Chen, W.-S. Hou [iD], Y. F. Liu, R.-S. Lu, E. Paganis, A. Psallidas, A. Steen

Department of Physics, Faculty of Science, Chulalongkorn University, Bangkok, Thailand
B. Asavapibhop [iD], N. Srimanobhas, N. Suwonjandee

Physics Department, Science and Art Faculty, Çukurova University, Adana, Turkey
A. Bat [iD], F. Boran, S. Cerci[50], S. Damarseckin, Z. S. Demiroglu [iD], F. Dolek, C. Dozen, I. Dumanoglu, E. Eskut,
G. Gokbulut, Y. Guler, E. Gurpinar, I. Hos[51], C. Isik, E. E. Kangal[52], O. Kara, A. Kayis Topaksu, U. Kiminsu [iD],
M. Oglakci [iD], G. Onengut, K. Ozdemir[53], A. Polatoz, D. Sunar Cerci[50], U. G. Tok, S. Turkcapar, I. S. Zorbakir [iD],
C. Zorbilmez

Physics Department, Middle East Technical University, Ankara, Turkey
B. Isildak[54], G. Karapinar[55], M. Yalvac, M. Zeyrek

Bogazici University, Istanbul, Turkey
I. O. Atakisi, E. Gülmez, M. Kaya[56], O. Kaya[57], S. Ozkorucuklu[58], S. Tekten, E. A. Yetkin [iD][59]

Istanbul Technical University, Istanbul, Turkey
M. N. Agaras [iD], A. Cakir [iD], K. Cankocak, Y. Komurcu, S. Sen [iD][60]

Institute for Scintillation Materials of National Academy of Science of Ukraine, Kharkov, Ukraine
B. Grynyov
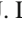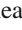
National Scientific Center, Kharkov Institute of Physics and Technology, Kharkov, Ukraine
L. Levchuk [iD]
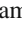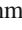
University of Bristol, Bristol, UK
F. Ball, J. J. Brooke [iD], D. Burns, E. Clement [iD], D. Cussans, O. Davignon, H. Flacher [iD], J. Goldstein [iD], G. P. Heath,
H. F. Heath [iD], L. Kreczko [iD], D. M. Newbold [iD][61], S. Paramesvaran, B. Penning [iD], T. Sakuma [iD], D. Smith, V. J. Smith,
J. Taylor, A. Titterton

Rutherford Appleton Laboratory, Didcot, UK
K. W. Bell, A. Belyaev [iD][62], C. Brew [iD], R. M. Brown, D. Cieri [iD], D. J. A. Cockerill, J. A. Coughlan, K. Harder, S. Harper,
J. Linacre [iD], K. Manolopoulos, E. Olaiya, D. Petyt, T. Schuh, C. H. Shepherd-Themistocleous, A. Thea [iD], I. R. Tomalin,
T. Williams, W. J. Womersley

Imperial College, London, UK
R. Bainbridge [iD], P. Bloch, J. Borg [iD], S. Breeze, O. Buchmuller, A. Bundock [iD], D. Colling, P. Dauncey [iD], G. Davies,
M. Della Negra, R. Di Maria, P. Everaerts [iD], G. Hall [iD], G. Iles, T. James, M. Komm [iD], C. Laner, L. Lyons,
A.-M. Magnan, S. Malik, A. Martelli [iD], J. Nash[63], A. Nikitenko[7], V. Palladino [iD], M. Pesaresi, D. M. Raymond,
A. Richards, A. Rose, E. Scott [iD], C. Seez, A. Shtipliyski, G. Singh, M. Stoye, T. Strebler [iD], S. Summers, A. Tapper [iD],
K. Uchida, T. Virdee [iD][17], N. Wardle [iD], D. Winterbottom, J. Wright, S. C. Zenz [iD]

Brunel University, Uxbridge, UK

J. E. Cole ⓘ, P. R. Hobson ⓘ, A. Khan, P. Kyberd ⓘ, C. K. Mackay, A. Morton ⓘ, I. D. Reid ⓘ, L. Teodorescu, S. Zahid

Baylor University, Waco, USA

K. Call, J. Dittmann, K. Hatakeyama, H. Liu, C. Madrid, B. McMaster, N. Pastika, C. Smith

Catholic University of America, Washington, DC, USA

R. Bartek ⓘ, A. Dominguez ⓘ

The University of Alabama, Tuscaloosa, USA

A. Buccilli ⓘ, S. I. Cooper, C. Henderson ⓘ, P. Rumerio, C. West

Boston University, Boston, USA

D. Arcaro, T. Bose, D. Gastler, S. Girgis, D. Pinna, C. Richardson, J. Rohlf, L. Sulak, D. Zou

Brown University, Providence, USA

G. Benelli, B. Burkle ⓘ, X. Coubez, D. Cutts ⓘ, M. Hadley, J. Hakala, U. Heintz, J. M. Hogan ⓘ [64], K. H. M. Kwok, E. Laird, G. Landsberg ⓘ, J. Lee, Z. Mao, M. Narain, S. Sagir ⓘ [65], R. Syarif ⓘ, E. Usai ⓘ, D. Yu

University of California, Davis, Davis, USA

R. Band, C. Brainerd ⓘ, R. Breedon, D. Burns, M. Calderon De La Barca Sanchez, M. Chertok, J. Conway, R. Conway, P. T. Cox, R. Erbacher, C. Flores, G. Funk, W. Ko, O. Kukral, R. Lander, M. Mulhearn, D. Pellett, J. Pilot, S. Shalhout, M. Shi, D. Stolp, D. Taylor ⓘ, K. Tos, M. Tripathi ⓘ, Z. Wang, F. Zhang

University of California, Los Angeles, USA

M. Bachtis, C. Bravo ⓘ, R. Cousins ⓘ, A. Dasgupta, S. Erhan, A. Florent ⓘ, J. Hauser ⓘ, M. Ignatenko, N. Mccoll, S. Regnard ⓘ, D. Saltzberg ⓘ, C. Schnaible, V. Valuev

University of California, Riverside, Riverside, USA

E. Bouvier ⓘ, K. Burt, R. Clare ⓘ, J. W. Gary ⓘ, S. M. A. Ghiasi Shirazi, G. Hanson, G. Karapostoli, E. Kennedy, F. Lacroix ⓘ, O. R. Long, M. Olmedo Negrete, M. I. Paneva, W. Si, L. Wang, H. Wei ⓘ, S. Wimpenny, B. R. Yates ⓘ

University of California, San Diego, La Jolla, USA

J. G. Branson, P. Chang, S. Cittolin, M. Derdzinski, R. Gerosa ⓘ, D. Gilbert ⓘ, B. Hashemi, A. Holzner ⓘ, D. Klein ⓘ, G. Kole ⓘ, V. Krutelyov ⓘ, J. Letts ⓘ, M. Masciovecchio, S. May, D. Olivito ⓘ, S. Padhi, M. Pieri ⓘ, V. Sharma ⓘ, M. Tadel, J. Wood, F. Würthwein ⓘ, A. Yagil ⓘ, G. Zevi Della Porta ⓘ

Department of Physics, University of California, Santa Barbara, Santa Barbara, USA

N. Amin, R. Bhandari ⓘ, C. Campagnari, M. Citron, V. Dutta, M. Franco Sevilla, L. Gouskos, R. Heller, J. Incandela ⓘ, H. Mei, A. Ovcharova, H. Qu ⓘ, J. Richman, D. Stuart, I. Suarez, S. Wang, J. Yoo

California Institute of Technology, Pasadena, USA

D. Anderson, A. Bornheim ⓘ, J. M. Lawhorn ⓘ, N. Lu ⓘ, H. B. Newman ⓘ, T. Q. Nguyen, J. Pata, M. Spiropulu ⓘ, J. R. Vlimant ⓘ, R. Wilkinson, S. Xie, Z. Zhang, R. Y. Zhu ⓘ

Carnegie Mellon University, Pittsburgh, USA

M. B. Andrews, T. Ferguson ⓘ, T. Mudholkar, M. Paulini ⓘ, M. Sun, I. Vorobiev, M. Weinberg
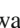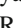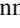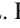
University of Colorado Boulder, Boulder, USA

J. P. Cumalat, W. T. Ford ⓘ, F. Jensen, A. Johnson, E. MacDonald, T. Mulholland, R. Patel, A. Perloff ⓘ, K. Stenson ⓘ, K. A. Ulmer ⓘ, S. R. Wagner ⓘ
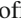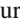
Cornell University, Ithaca, USA

J. Alexander, J. Chaves ⓘ, Y. Cheng, J. Chu, A. Datta, K. Mcdermott ⓘ, N. Mirman, J. R. Patterson ⓘ, D. Quach ⓘ, A. Rinkevicius ⓘ, A. Ryd, L. Skinnari ⓘ, L. Soffi ⓘ, S. M. Tan, Z. Tao, J. Thom, J. Tucker ⓘ, P. Wittich ⓘ, M. Zientek

Fermi National Accelerator Laboratory, Batavia, USA
S. Abdullin, M. Albrow, M. Alyari, G. Apollinari, A. Apresyan, A. Apyan, S. Banerjee, L. A. T. Bauerdick,
A. Beretvas, J. Berryhill, P. C. Bhat, K. Burkett, J. N. Butler, A. Canepa, G. B. Cerati, H. W. K. Cheung,
F. Chlebana, M. Cremonesi, J. Duarte, V. D. Elvira, J. Freeman, Z. Gecse, E. Gottschalk, L. Gray, D. Green,
S. Grünendahl, O. Gutsche, J. Hanlon, R. M. Harris, S. Hasegawa, J. Hirschauer, Z. Hu, B. Jayatilaka, S. Jindariani,
M. Johnson, U. Joshi, B. Klima, M. J. Kortelainen, B. Kreis, S. Lammel, D. Lincoln, R. Lipton, M. Liu,
T. Liu, J. Lykken, K. Maeshima, J. M. Marraffino, D. Mason, P. McBride, P. Merkel, S. Mrenna, S. Nahn, V. O'Dell,
K. Pedro, C. Pena, O. Prokofyev, G. Rakness, F. Ravera, A. Reinsvold, L. Ristori, A. Savoy-Navarro[66],
B. Schneider, E. Sexton-Kennedy, A. Soha, W. J. Spalding, L. Spiegel, S. Stoynev, J. Strait, N. Strobbe,
L. Taylor, S. Tkaczyk, N. V. Tran, L. Uplegger, E. W. Vaandering, C. Vernieri, M. Verzocchi, R. Vidal,
M. Wang, H. A. Weber

University of Florida, Gainesville, USA
D. Acosta, P. Avery, P. Bortignon, D. Bourilkov, A. Brinkerhoff, L. Cadamuro, A. Carnes, D. Curry, R. D. Field,
S. V. Gleyzer, B. M. Joshi, J. Konigsberg, A. Korytov, K. H. Lo, P. Ma, K. Matchev, N. Menendez, G. Mitselmakher,
D. Rosenzweig, K. Shi, D. Sperka, J. Wang, S. Wang, X. Zuo
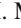
Florida International University, Miami, USA
Y. R. Joshi, S. Linn

Florida State University, Tallahassee, USA
A. Ackert, T. Adams, A. Askew, S. Hagopian, V. Hagopian, K. F. Johnson, T. Kolberg, G. Martinez, T. Perry,
H. Prosper, A. Saha, C. Schiber, R. Yohay

Florida Institute of Technology, Melbourne, USA
M. M. Baarmand, V. Bhopatkar, S. Colafranceschi, M. Hohlmann, D. Noonan, M. Rahmani, T. Roy, M. Saunders,
F. Yumiceva

University of Illinois at Chicago (UIC), Chicago, USA
M. R. Adams, L. Apanasevich, D. Berry, R. R. Betts, R. Cavanaugh, X. Chen, S. Dittmer, O. Evdokimov,
C. E. Gerber, D. A. Hangal, D. J. Hofman, K. Jung, J. Kamin, C. Mills, M. B. Tonjes, N. Varelas, H. Wang,
X. Wang, Z. Wu, J. Zhang

The University of Iowa, Iowa City, USA
M. Alhusseini, B. Bilki[67], W. Clarida, K. Dilsiz[68], S. Durgut, R. P. Gandrajula, M. Haytmyradov, V. Khristenko,
J.-P. Merlo, A. Mestvirishvili, A. Moeller, J. Nachtman, H. Ogul[69], Y. Onel, F. Ozok[70], A. Penzo, C. Snyder, E. Tiras,
J. Wetzel

Johns Hopkins University, Baltimore, USA
B. Blumenfeld, A. Cocoros, N. Eminizer, D. Fehling, L. Feng, A. V. Gritsan, W. T. Hung, P. Maksimovic,
J. Roskes, U. Sarica, M. Swartz, M. Xiao

The University of Kansas, Lawrence, USA
A. Al-bataineh, P. Baringer, A. Bean, S. Boren, J. Bowen, A. Bylinkin, J. Castle, S. Khalil, A. Kropivnitskaya,
D. Majumder, W. Mcbrayer, M. Murray, C. Rogan, S. Sanders, E. Schmitz, J. D. Tapia Takaki, Q. Wang

Kansas State University, Manhattan, USA
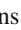S. Duric, A. Ivanov, K. Kaadze, D. Kim, Y. Maravin, D. R. Mendis, T. Mitchell, A. Modak, A. Mohammadi

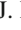**Lawrence Livermore National Laboratory, Livermore, USA**
F. Rebassoo, D. Wright

University of Maryland, College Park, USA
A. Baden, O. Baron, A. Belloni, S. C. Eno, Y. Feng, C. Ferraioli, N. J. Hadley, S. Jabeen, G. Y. Jeng, R. G. Kellogg,
J. Kunkle, A. C. Mignerey, S. Nabili, F. Ricci-Tam, M. Seidel, Y. H. Shin, A. Skuja, S. C. Tonwar, K. Wong

Massachusetts Institute of Technology, Cambridge, USA

D. Abercrombie, B. Allen ⓘ, V. Azzolini, A. Baty ⓘ, R. Bi, S. Brandt, W. Busza ⓘ, I. A. Cali, M. D'Alfonso ⓘ, Z. Demiragli, G. Gomez Ceballos, M. Goncharov, P. Harris, D. Hsu, M. Hu, Y. Iiyama ⓘ, M. Klute, D. Kovalskyi ⓘ, Y.-J. Lee ⓘ, P. D. Luckey, B. Maier, A. C. Marini ⓘ, C. Mcginn, C. Mironov, S. Narayanan ⓘ, X. Niu, C. Paus, D. Rankin, C. Roland, G. Roland, Z. Shi ⓘ, G. S. F. Stephans ⓘ, K. Sumorok, K. Tatar ⓘ, D. Velicanu, J. Wang, T. W. Wang, B. Wyslouch ⓘ

University of Minnesota, Minneapolis, USA

A. C. Benvenuti[†], R. M. Chatterjee, A. Evans ⓘ, P. Hansen, J. Hiltbrand, Sh. Jain ⓘ, S. Kalafut, M. Krohn, Y. Kubota, Z. Lesko, J. Mans ⓘ, R. Rusack, M. A. Wadud

University of Mississippi, Oxford, USA

J. G. Acosta, S. Oliveros ⓘ

University of Nebraska-Lincoln, Lincoln, USA

E. Avdeeva, K. Bloom ⓘ, D. R. Claes, C. Fangmeier, F. Golf ⓘ, R. Gonzalez Suarez, R. Kamalieddin, I. Kravchenko ⓘ, J. Monroy ⓘ, J. E. Siado, G. R. Snow, B. Stieger

State University of New York at Buffalo, Buffalo, USA

A. Godshalk, C. Harrington, I. Iashvili ⓘ, A. Kharchilava, C. Mclean, D. Nguyen, A. Parker, S. Rappoccio ⓘ, B. Roozbahani
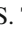
Northeastern University, Boston, USA

G. Alverson ⓘ, E. Barberis, C. Freer, Y. Haddad ⓘ, A. Hortiangtham, G. Madigan, D. M. Morse ⓘ, T. Orimoto, A. Tishelman-charny, T. Wamorkar, B. Wang, A. Wisecarver, D. Wood ⓘ

Northwestern University, Evanston, USA

S. Bhattacharya, J. Bueghly, O. Charaf, T. Gunter, K. A. Hahn, N. Odell, M. H. Schmitt ⓘ, K. Sung, M. Trovato ⓘ, M. Velasco

University of Notre Dame, Notre Dame, USA

R. Bucci, N. Dev ⓘ, R. Goldouzian, M. Hildreth, K. Hurtado Anampa, C. Jessop, D. J. Karmgard, K. Lannon, W. Li, N. Loukas ⓘ, N. Marinelli, F. Meng, C. Mueller, Y. Musienko[39], M. Planer, R. Ruchti, P. Siddireddy, G. Smith, S. Taroni ⓘ, M. Wayne, A. Wightman, M. Wolf ⓘ, A. Woodard

The Ohio State University, Columbus, USA

J. Alimena ⓘ, L. Antonelli, B. Bylsma, L. S. Durkin, S. Flowers, B. Francis, C. Hill ⓘ, W. Ji, T. Y. Ling, W. Luo, B. L. Winer

Princeton University, Princeton, USA

S. Cooperstein, P. Elmer ⓘ, J. Hardenbrook, N. Haubrich, S. Higginbotham, A. Kalogeropoulos ⓘ, S. Kwan, D. Lange, M. T. Lucchini ⓘ, J. Luo, D. Marlow ⓘ, K. Mei ⓘ, I. Ojalvo, J. Olsen ⓘ, C. Palmer, P. Piroué, J. Salfeld-Nebgen ⓘ, D. Stickland ⓘ, C. Tully ⓘ

University of Puerto Rico, Mayaguez, USA

S. Malik ⓘ, S. Norberg

Purdue University, West Lafayette, USA

A. Barker, V. E. Barnes ⓘ, S. Das, L. Gutay, M. Jones, A. W. Jung ⓘ, A. Khatiwada, B. Mahakud, D. H. Miller, N. Neumeister ⓘ, C. C. Peng, S. Piperov ⓘ, H. Qiu, J. F. Schulte ⓘ, J. Sun ⓘ, F. Wang, R. Xiao, W. Xie

Purdue University Northwest, Hammond, USA

T. Cheng, J. Dolen, N. Parashar

Rice University, Houston, USA

Z. Chen ⓘ, K. M. Ecklund ⓘ, S. Freed, F. J. M. Geurts ⓘ, M. Kilpatrick, Arun Kumar, W. Li, B. P. Padley ⓘ, R. Redjimi, J. Roberts, J. Rorie, W. Shi ⓘ, Z. Tu ⓘ, A. Zhang

University of Rochester, Rochester, USA

A. Bodek, P. de Barbaro, R. Demina, Y.t. Duh, J. L. Dulemba, C. Fallon, T. Ferbel, M. Galanti, A. Garcia-Bellido, J. Han, O. Hindrichs, A. Khukhunaishvili, E. Ranken, P. Tan, R. Taus

The Rockefeller University, New York, USA

R. Ciesielski, K. Goulianos

Rutgers, The State University of New Jersey, Piscataway, USA

B. Chiarito, J. P. Chou, Y. Gershtein, E. Halkiadakis, A. Hart, M. Heindl, E. Hughes, S. Kaplan, R. Kunnawalkam Elayavalli, S. Kyriacou, I. Laflotte, A. Lath, R. Montalvo, K. Nash, M. Osherson, H. Saka, S. Salur, S. Schnetzer, D. Sheffield, S. Somalwar, R. Stone, S. Thomas, P. Thomassen

University of Tennessee, Knoxville, USA

H. Acharya, A. G. Delannoy, J. Heideman, G. Riley, S. Spanier

Texas A&M University, College Station, USA

O. Bouhali[71], A. Celik, M. Dalchenko, M. De Mattia, A. Delgado, S. Dildick, R. Eusebi, J. Gilmore, T. Huang, T. Kamon[72], S. Luo, D. Marley, R. Mueller, D. Overton, L. Perniè, D. Rathjens, A. Safonov

Texas Tech University, Lubbock, USA

N. Akchurin, J. Damgov, F. De Guio, P. R. Dudero, S. Kunori, K. Lamichhane, S. W. Lee, T. Mengke, S. Muthumuni, T. Peltola, S. Undleeb, I. Volobouev, Z. Wang, A. Whitbeck

Vanderbilt University, Nashville, USA

S. Greene, A. Gurrola, R. Janjam, W. Johns, C. Maguire, A. Melo, H. Ni, K. Padeken, F. Romeo, P. Sheldon, S. Tuo, J. Velkovska, M. Verweij, Q. Xu
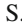
University of Virginia, Charlottesville, USA

M. W. Arenton, P. Barria, B. Cox, R. Hirosky, M. Joyce, A. Ledovskoy, H. Li, C. Neu, T. Sinthuprasith, Y. Wang, E. Wolfe, F. Xia

Wayne State University, Detroit, USA

R. Harr, P. E. Karchin, N. Poudyal, J. Sturdy, P. Thapa, S. Zaleski

University of Wisconsin-Madison, Madison, WI, USA

J. Buchanan, C. Caillol, D. Carlsmith, S. Dasu, I. De Bruyn, L. Dodd, B. Gomber[73], M. Grothe, M. Herndon, A. Hervé, U. Hussain, P. Klabbers, A. Lanaro, K. Long, R. Loveless, T. Ruggles, A. Savin, V. Sharma, N. Smith, W. H. Smith, N. Woods

† **Deceased**

1: Also at Vienna University of Technology, Vienna, Austria
2: Also at IRFU, CEA, Université Paris-Saclay, Gif-sur-Yvette, France
3: Also at Universidade Estadual de Campinas, Campinas, Brazil
4: Also at Federal University of Rio Grande do Sul, Porto Alegre, Brazil
5: Also at Université Libre de Bruxelles, Brussels, Belgium
6: Also at University of Chinese Academy of Sciences, Beijing, China
7: Also at Institute for Theoretical and Experimental Physics named by A.I. Alikhanov of NRC 'Kurchatov Institute', Moscow, Russia
8: Also at Joint Institute for Nuclear Research, Dubna, Russia
9: Now at Cairo University, Cairo, Egypt
10: Also at Fayoum University, El-Fayoum, Egypt
11: Now at British University in Egypt, Cairo, Egypt
12: Now at Ain Shams University, Cairo, Egypt
13: Also at Department of Physics, King Abdulaziz University, Jeddah, Saudi Arabia
14: Also at Université de Haute Alsace, Mulhouse, France
15: Also at Skobeltsyn Institute of Nuclear Physics, Lomonosov Moscow State University, Moscow, Russia
16: Also at Tbilisi State University, Tbilisi, Georgia

17: Also at CERN, European Organization for Nuclear Research, Geneva, Switzerland

18: Also at RWTH Aachen University, III. Physikalisches Institut A, Aachen, Germany

19: Also at University of Hamburg, Hamburg, Germany

20: Also at Brandenburg University of Technology, Cottbus, Germany

21: Also at Institute of Physics, University of Debrecen, Debrecen, Hungary, Debrecen, Hungary

22: Also at Institute of Nuclear Research ATOMKI, Debrecen, Hungary

23: Also at MTA-ELTE Lendület CMS Particle and Nuclear Physics Group, Eötvös Loránd University, Budapest, Hungary, Budapest, Hungary

24: Also at IIT Bhubaneswar, Bhubaneswar, India

25: Also at Institute of Physics, Bhubaneswar, India

26: Also at Shoolini University, Solan, India

27: Also at University of Visva-Bharati, Santiniketan, India

28: Also at Isfahan University of Technology, Isfahan, Iran

29: Also at Plasma Physics Research Center, Science and Research Branch, Islamic Azad University, Tehran, Iran

30: Also at Italian National Agency for New Technologies, Energy and Sustainable Economic Development, Bologna, Italy

31: Also at Università degli Studi di Siena, Siena, Italy

32: Also at Scuola Normale e Sezione dell'INFN, Pisa, Italy

33: Also at Department of Physics, Kyung Hee University, Seoul, Korea

34: Also at Riga Technical University, Riga, Latvia

35: Also at International Islamic University of Malaysia, Kuala Lumpur, Malaysia

36: Also at Malaysian Nuclear Agency, MOSTI, Kajang, Malaysia

37: Also at Consejo Nacional de Ciencia y Tecnología, Mexico City, Mexico

38: Also at Warsaw University of Technology, Institute of Electronic Systems, Warsaw, Poland

39: Also at Institute for Nuclear Research, Moscow, Russia

40: Now at National Research Nuclear University 'Moscow Engineering Physics Institute' (MEPhI), Moscow, Russia

41: Also at St. Petersburg State Polytechnical University, St. Petersburg, Russia

42: Also at University of Florida, Gainesville, USA

43: Also at Budker Institute of Nuclear Physics, Novosibirsk, Russia

44: Also at Faculty of Physics, University of Belgrade, Belgrade, Serbia

45: Also at University of Belgrade, Faculty of Physics and VINCA Institute of Nuclear Sciences, Belgrade, Serbia

46: Also at INFN Sezione di Pavia ^{a}, Università di Pavia ^{b}, Pavia, Italy

47: Also at National and Kapodistrian University of Athens, Athens, Greece

48: Also at Universität Zürich, Zurich, Switzerland

49: Also at Stefan Meyer Institute for Subatomic Physics, Vienna, Austria

50: Also at Adiyaman University, Adiyaman, Turkey

51: Also at Istanbul Aydin University, Application and Research Center for Advanced Studies (App. & Res. Cent. for Advanced Studies), Istanbul, Turkey

52: Also at Mersin University, Mersin, Turkey

53: Also at Piri Reis University, Istanbul, Turkey

54: Also at Ozyegin University, Istanbul, Turkey

55: Also at Izmir Institute of Technology, Izmir, Turkey

56: Also at Marmara University, Istanbul, Turkey

57: Also at Kafkas University, Kars, Turkey

58: Also at Istanbul University, Istanbul, Turkey

59: Also at Istanbul Bilgi University, Istanbul, Turkey

60: Also at Hacettepe University, Ankara, Turkey

61: Also at Rutherford Appleton Laboratory, Didcot, UK

62: Also at School of Physics and Astronomy, University of Southampton, Southampton, UK

63: Also at Monash University, Faculty of Science, Clayton, Australia

64: Also at Bethel University, St. Paul, Minneapolis, USA, St. Paul, USA

65: Also at Karamanoğlu Mehmetbey University, Karaman, Turkey

66: Also at Purdue University, West Lafayette, USA

67: Also at Beykent University, Istanbul, Turkey, Istanbul, Turkey

68: Also at Bingol University, Bingol, Turkey

69: Also at Sinop University, Sinop, Turkey

70: Also at Mimar Sinan University, Istanbul, Istanbul, Turkey

71: Also at Texas A&M University at Qatar, Doha, Qatar

72: Also at Kyungpook National University, Daegu, Korea, Daegu, Korea

73: Also at University of Hyderabad, Hyderabad, India

TOTEM Collaboration

G. Antchev[a], P. Aspell[9], I. Atanassov[a], V. Avati[7,9], J. Baechler[9], C. Baldenegro Barrera[11], V. Berardi[4a,4b], M. Berretti[2a], V. Borchsh[8], E. Bossini[6b,9], U. Bottigli[6b], M. Bozzo[5a,5b], H. Burkhardt[9], F. S. Cafagna[4a], M. G. Catanesi[4a], M. Csanád[3a,b], T. Csörgő[3a,3b], M. Deile[9], F. De Leonardis[4a,4c], M. Doubek[1c], D. Druzhkin[8,9], K. Eggert[10], V. Eremin[d], A. Fiergolski[9], L. Forthomme[2a,2b], F. Garcia[2a], V. Georgiev[1a], S. Giani[9], L. Grzanka[7], J. Hammerbauer[1a], T. Isidori[11], V. Ivanchenko[8], M. Janda[1c], A. Karev[9], J. Kašpar[1b,9], B. Kaynak[1e], J. Kopal[9], V. Kundrát[1b], S. Lami[6a], R. Linhart[1a], C. Lindsey[11], M. V. Lokajíček[1b,†], L. Losurdo[6b], F. Lucas Rodríguez[9], M. Macrí[5a], M. Malawski[7], N. Minafra[11], S. Minutoli[5a], T. Naaranoja[2a,2b], F. Nemes[3a,9], H. Niewiadomski[10], T. Novák[3b], E. Oliveri[9], F. Oljemark[2a,2b], M. Oriunno[f], K. Österberg[2a,2b], P. Palazzi[9], V. Passaro[4c,4a], Z. Peroutka[1a], J. Procházka[1b], M. Quinto[4a,4b], E. Radermacher[9], E. Radicioni[4a], F. Ravotti[9], C. Royon[11], G. Ruggiero[9], H. Saarikko[2a,2b], V. D. Samoylenko[c], A. Scribano[6a], J. Siroky[1a], J. Smajek[9], W. Snoeys[9], R. Stefanovitch[9], J. Sziklai[3a], C. Taylor[10], E. Tcherniaev[8], N. Turini[6b], O. Urban[1a], V. Vacek[1c], O. Vavroch[1a], J. Welti[2a,2b], J. Williams[11], J. Zich[1a], K. Zielinski[7]

1 [a]University of West Bohemia, Pilsen, Czech Republic, [b]Institute of Physics of the Academy of Sciences of the Czech Republic, Prague, Czech Republic, [c]Czech Technical University, Prague, Czech Republic

2 [a]Helsinki Institute of Physics, University of Helsinki, Helsinki, Finland, [b]Department of Physics, University of Helsinki, Helsinki, Finland

3 [a]Wigner Research Centre for Physics, RMKI, Budapest, Hungary, [b]EKU KRC, Gyöngyös, Hungary

4 [a]INFN Sezione di Bari, Bari, Italy, [b]Dipartimento Interateneo di Fisica di Bari, Bari, Italy, [c]Dipartimento di Ingegneria Elettrica e dell'Informazione, Politecnico di Bari, Bari, Italy

5 [a]INFN Sezione di Genova, Genoa, Italy, [b]Università degli Studi di Genova, Genoa, Italy

6 [a]INFN Sezione di Pisa, Pisa, Italy, [b]Università degli Studi di Siena and Gruppo Collegato INFN di Siena, Siena, Italy

7 AGH University of Science and Technology, Krakow, Poland

8 Tomsk State University, Tomsk, Russia

9 CERN, Geneva, Switzerland

10 Department of Physics, Case Western Reserve University, Cleveland, OH, USA

11 The University of Kansas, Lawrence, USA

[a]INRNE-BAS, Institute for Nuclear Research and Nuclear Energy, Bulgarian Academy of Sciences, Sofia, Bulgaria.

[b]Department of Atomic Physics, ELTE University, Budapest, Hungary.

[c]NRC 'Kurchatov Institute'-IHEP, Protvino, Russia.

[d]Ioffe Physical-Technical Institute of Russian Academy of Sciences, St. Petersburg, Russian Federation.

[e]Istanbul University, Istanbul, Turkey.

[f]SLAC National Accelerator Laboratory, Stanford, CA, USA.

[†] Deceased